Universidad de Sonora

División de Ciencias Exactas y Naturales

Departamento de Investigación en Física

Initial conditions for a boosted black hole in the CTT approach

por

José Abraham Arvizu Valenzuela

Una tesis presentada a la Universidad de Sonora

para la obtención del Grado de

Maestro en Ciencias (Física)

Dirigida por:

Dr. Carlos A. Calcáneo Roldán

Universidad de Sonora

Hermosillo, Sonora México

Febrero 2018

Agradecimientos

Agradezco a mis padres y hermanos por apoyarme de manera incondicional a través del desarrollo de este trabajo. Sin todo su cariño y comprensión no lo habría logrado.

Gracias a CONACYT por el apoyo económico recibido para realizar mis estudios de posgrado.

A mis amigos fuera de los cubos. Ese pequeño grupo de personas que me hacen reir y preocuparme por ellos. Aunque no ayudaron de manera directa sobre el trabajo estuvieron ahí para levantarme el ánimo.

A mis amigos dentro de los cubos. Este aún más reducido grupo de personas que me han brindado su amistad y cálido cariño.

Maura, gracias por tu apoyo en la redacción y revisión del trabajo. Como nos reimos con las tonterias como "On the other hand." ...

Dupret, es la onda poder trabajar en un lugar donde estes cómodo; tal como escuchar desde Rhapsody hasta Eminem o comer pizzas gigantes y platicar de cosas numéricas. Gracias man.

The doctor!, gracias por aguanar my obstinada forma de trabajar. Eso de poder llegar al límite en una discusión y al dia siguiente reirnos como en una semana atrás, es raro de encontrar.

Profe Malena, gracias por siempre estar dispuesta a ayudarme.

Sandra, gracias por los chocolates y los consejos de mamá. Perdón por tu llave!

Oscar, gracias por la amistad man, por los consejos raros y la cura.

Cobos, gracias por la amistad y apoyarme en este proceso.

Gracias a todos ustedes que me han ayudado a lo largo de esta etapa de mi vida.

Gracias Karen, por estar en buenas y malas, por ser una amiga y más.

Contents

Figures list

Introduction

From its inception, General Relativity has been subject of a wide range of experimental scrutiny. Among the most successful of which are: the deviation of light in the prolonged solar eclipse of Saros 1919 [DED20], the anomalous precession of Mercury's perihelion, the change of frequency of the binary system PSR B1913+16 (proving the existence of gravitational radiation [TW89]), recent gravitational probes [GP-a, GP-b] that have proven, to second order, the existence of spacetime as the underlying fabric of the Universe and the recent direct detection of gravitational waves [AAA$^+$16].

At present, there is much work which bases its results on General Relativity:

- The Cosmological standard model, ΛCDM, and its variations.
    - Baryonic acoustic oscillations (*BAO*).
    - Structure formation in the Universe.
    - The very existence of a cosmological constant and the associated cosmological acceleration.
- Lienearised General relativity and gravitational waves.

all of which are related to solutions to Einsteins equations for the gravitational field.

At the present level of accuracy there is a wealth of observations that are yet to be completely understood. For example, the fluctuations measured by *WMAP* of the order of 10^{-5} in the anisotropies of the BAO [BH10].

With the new era of gravitational wave detection and gravitational wave Astronomy, the need for second (or even third!) order results will be of great importance. As is well known, the field equations are a system of coupled nonlinear partial differential equations and therefore quantitative results will only be achieved by direct numerical solutions.

The main goal of this work is to take us from a knowledge of the Theory of General Relativity (GR) to a basic level in Numerical Relativity (NR). This includes the basic background and knowledge needed to reproduce contemporary literature, in particular we reproduce [IB09].

This work discusses the problem of obtaining the initial conditions for a "Boosted Black Hole". This is, we find the spacetime geometry around a black hole at a given time, when the black hole moves with linear momentum $\vec{P}$, in some reference frame. This may be of use when discussing the interaction of black holes, as in the colission of two stellar compact objects.

Although the work does not represent original ideas on the theory of numerical relativity, it compiles some points of view from the referenced authors and contains many calculations left to the reader. At the same time, there is plenty of room to extend this work to further calculations.

After this brief introduction, chapter 1 is a general introduction to Numerical Relativity, in particular 3+1 NR. Chapter 2 explains the use of a particular gauge and coordinate choice which is used frequently in the literature and chapter 3 represents the solution to the problem presented in [IB09]. In the last section we finish with some concluding remarks.

Chapter 1 | *3+1 General relativity*

In a relatively short time more systems which can be described by means of GR have been found. This brings about the need for more precise calculations for those systems. However, to solve Einstein's equations for a specific system means we must deal with a set of coupled non-linear Partial Differential Equations (PDE). In order to obtain those solutions in an easy way, GR has been reformulated to the 3+1 relativity.

1.1 3D-metric

The basic idea of 3+1 relativity is the usage that Einstein's equations have derivatives on the metric at most in second order. This, in addition to one of Bianchi's identities, leads to a set of equations which is preserved through any temporal change. Since these equations are valid for any time we could freely designate a time origin. Thus, for discrete values of time we have as many sets of equations as time values, but just one set for the origin. Because of these are given at fixed times they are called spatial *constraint equations*. Therefore, the equations corresponding to the origin will help us to obtain the initial value for the metric tensor.

The Bianchi identity that we mentioned above is [MTW73]

$$\nabla_b G^{ab} = \nabla_b \left(R^{ab} - \frac{1}{2} R g^{ab} \right) = 8\pi \nabla_b T^{ab} = 0 \,. \tag{1.1}$$

Where we used the notation and conventions described in the appendix A. If we take the $a = 0 \equiv t$ component, the left hand side (LHS) involves only one term with an explicit time-derivative on Einstein's tensor, hence a third order on the metric, g^{ab}:

$$\partial_t G^{a0} = - \left(\partial_i G^{ai} + G^{bc} \Gamma^a_{\ bc} + G^{ab} \Gamma^c_{\ bc} \right) .$$

The Right Hand Side (RHS) of this equation does not have an explicit time-derivative, therefore at up to a second order on the metric, and hence the four quantities G^{a0} must not contain second order time-derivatives on the metric.

From classical problems we know that is enough to give the values for positions and velocities at certain time. Usually we have to seek for an expression containing second order time-derivatives on positions, integrate it and use the initial values to solve for positions and velocities. In general relativity's formalism this is slightly different. Since positions do not have an absolute meaning here, we have to look for the zero and first order of time-derivatives on the metric.

The above means that, as G^{a0} do not contain second order time-derivatives on the metric, we are not able to inquire any information about the dynamics of the spacetime. Nevertheless, these give us information about what conditions the dynamics must obey. No matter what it is, G^{a0} persist as the system evolves in time. This encourages us to look for expressions that carry on those constraint equations through the whole time evolution of the metric.

Then, in 3+1 relativity, it's permitted to choose an arbitrary origin for time which leaves an initial spatial 3D-sheet $\mathcal{T}_o$ to be determined. Once $\mathcal{T}_o$ is specified, it could be evolved in time with the rest of the equations, others than G^{a0}, to the next 3D-sheet $\mathcal{T}$ and so on. Thus, we obtain a time ordered foliation of spatial sheets $\mathcal{T}$.

We have already outlined a logical procedure to solve Einstein's equations. Clearly, it is not enough only to notice that time and space have been separated. In order to begin the reformulation of general relativity, we assume that the foliations $\mathcal{T}$ could be ordered by a global parameter, namely global time t. Then we pick an unitary time-like vector, n^a, being this the gradient of the scalar field t

$$n^a \equiv -\alpha g^{ab}\nabla_b t \quad ; \qquad (\alpha)^{-2} \equiv -g^{ab}\nabla_a t \nabla_b t \,, \tag{1.2}$$

where α makes n^a unitary and time-like

$$n^a n_a = \alpha^2 g^{ab}\nabla_a t \nabla_b t = -1 \,. \tag{1.3}$$

t is not necessarily the time of a coordinate set, but there is a connection with it which will be clearer below. Since n^a is time-like and orthogonal to any spatial sheet, $\mathcal{T}$, a spatial projector could be associated to it

$$\gamma_a^b = g_a^b + n_a n^b \,. \tag{1.4}$$

E.g., projecting any vector to these spatial 3D-sheets would be orthogonal to $\vec{n}$:

$$\gamma_a^b v^a \equiv \perp v^b = \left(g_a^b + n_a n^b\right) v^a = v^b + n_a v^a n^b$$
$$n_b \perp v^b = v^b n_b + n_a v^a n^b n_b = v^b n_b - n_a v^a = 0 \,.$$

However, if the vector is time-like its projection is null:

$$\gamma_a^b n^a = \left(g_a^b + n_a n^b\right) n^a = n^b - n^b = 0 \,. \tag{1.5}$$

The definition of α in (1.2) makes it a graduation measure of $\vec{n}$; is worth to remember that it is a scalar field, changing in general, at every point of the spacetime. So α measures the separation between foliations along a time-like vector on which the evolution is being developed. As we note in figure (1.1) for the case of α = constant, foliations $\mathcal{T}$ are carried parallel to themselves in equal intervals of α. However, the lapse, α, is in general a function with different value at every spatial point of $\mathcal{T}$. In such case, foliations would be evolving with different shapes. Moreover, if α could change with time, the 3D-sheets would evolve in even a more complicated way. Then, it is important to choose a proper lapse function.

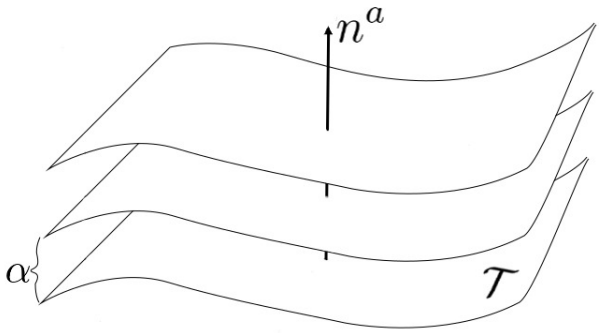

Figure 1.1: Foliation of different $\mathcal{T}$'s along n^a with the lapse function α = constant.

We can choose this function arbitrarily, however, it plays an important role for numerical developments. We discuss more about this in chapter 2. For now, let's put our attention on the definition (1.4). The symbol γ_a^b is a bridge from spacetime in a 4D-manifold $\mathcal{M}$ to a reduced spacetime $\mathcal{T}$ in a 3D-manifold. Properly speaking, $\mathcal{T}$ exists in $\mathcal{M}$ as an embedded sheet from an actual 3D-space, they are continuous and mapped one-to-one. This implies that $\mathcal{T}$ does not intersect itself [Gou07].

The scalar field t, defines level curves (discrete values of it) which are these $\mathcal{T}$. In such way, this 3D-space is our everyday living 3D-space, while $\mathcal{T}$ is part of the solution to Einstein's equations. For example, if the Cartesian coordinates set is chosen, then a point in $\mathcal{T}$ will have (t, x, y, z) coordinates.

Nonetheless, γ_a^b is much more than a bridge, we have seen how it works as an orthogonal projector to $\vec{n}$. However, if we thought it as a rank 2 covariant tensor, e.g., by taking down its upper index:

$$\gamma_{ab} = g_{bc}\gamma_a^c = g_{ab} + n_a n_b \,, \tag{1.6}$$

it would only measure the spatial part in the spacetime objects. Thus, the application of γ_{ab} on a time-like vector leads to zero. Let's suppose that l^a is a time-like vector. In that case it's proportional to n^a for any factor w, then

$$\gamma_{ab}l^a l^b = w^2 n^a n_b + w^2 n^a n_a n^b n_b = 0 \,.$$

Otherwise $\gamma_{ab}l^a l^b$ would lead to l^2. As a result, γ_{ab} is proposed as the 3D-metric tensor or induced metric. It measures the spacetime distance on any $\mathcal{T}$ and hence it keeps the $\mathcal{T}$'s geometry.

From the previous, we notice that for some space-like vectors $\vec{u}$ and $\vec{v}$, it follows that:

$$g\left(\vec{u}, \vec{v}\right) = \gamma\left(\vec{u}, \vec{v}\right) . \tag{1.7}$$

Therefore, g_{ij} and γ_{ij} keep the same information on the spatial part of the spacetime objects, i.e.,

$$g_{ij} = \gamma_{ij} \,. \tag{1.8}$$

However, since the $\mathcal{T}$ foliations could change along $\vec{n}$, we stress that remaining components have different relationships among them.

1.2 Extrinsic curvature

In order to describe the spacetime via this 3D-metric, we have to describe $\mathcal{T}$ and how it changes along $\vec{n}$. To do so, a first approach may be to describe changes in $\mathcal{T}$ respect to time (t field). However, doing this by means of the curvature tensor, as in Einstein's equations, has the following issue. The Riemann tensor contains information about spacetime and not space nor time separated. So, using it to describe changes in $\mathcal{T}$ will not be advantageous, it would be the same thing as trying to solve directly Einstein's equations.

A better way, is to describe the foliations using the extrinsic curvature tensor. It describes the geometry of $\mathcal{T}$ as embedded in the outer spacetime. Thus, the extrinsic curvature tensor already has the information about space and time separated.

In order to write the extrinsic curvature tensor, we have to take the change of $\vec{n}$ at successive foliations and then project it on $\mathcal{T}$ [BS10]. To do so, we need to define the spatial covariant derivative. Just as those vectors already projected with (1.4), the covariant derivative has its projected form. E.g. for a 2-rank tensor W^c_b, $\binom{1}{1}$, it follows that

$$D_a W^c_b \equiv \gamma^r_b \gamma^c_q \gamma^s_a \nabla_s W^q_r \,. \tag{1.9}$$

And so on for $\binom{n}{m}$-rank tensors. From (1.9), we can see that the commutativity between ∇_a and g_{bc} is inherited to D_a and γ_{bc} :

$$\begin{aligned} D_a\gamma_{bc} &= \gamma_b^r\gamma_c^q\gamma_a^s\nabla_s\gamma_{qr} \\ &= \gamma_b^r\gamma_c^q\gamma_a^s\nabla_s\left(g_{qr}+n_q n_r\right) \\ D_a\gamma_{bc} &= 0\,. \end{aligned} \tag{1.10}$$

Where we used (1.5). Notice that (1.9) implies the projection of objects defined by derivative operators like gradient and Christoffel symbol, Riemann and Ricci tensors, etc. For example, for a 4D-vector v^b, its 3D-covariant derivative would be

$$D_d v^e = \gamma_d^a\gamma_b^e\nabla_a v^b = \gamma_d^a\gamma_b^e\left(\partial_a v^b + v^c\Gamma^b{}_{ac}\right)\,, \tag{1.11}$$

with v^c lying in $\mathcal{T}$. Thus, rewriting $v^c = \gamma_q^c v^q$ we can interpret the second term of (1.11) as our projected Christoffel symbols, $\gamma_q^c\gamma_d^a\gamma_b^e\Gamma^b{}_{ac}$. Indeed, if we use (1.6) and the 3D-partial derivatives as given in the first term of (1.11) we could express them as

$$\Gamma^e{}_{dq} = \frac{1}{2}\gamma^{ef}\left(\partial_d\gamma_{fq}+\partial_q\gamma_{fd}-\partial_f\gamma_{dq}\right)\,. \tag{1.12}$$

This similarity of the 3D-Christoffel symbols to their respective 4D expressions has a repercussion on the 3D-Riemman tensor and its contractions. The 3D-Riemann tensor is given by

$$R_{abc}{}^d = \partial_b\Gamma^d{}_{ac} - \partial_a\Gamma^d{}_{bc} + \Gamma^e{}_{ac}\Gamma^d{}_{eb} - \Gamma^e{}_{bc}\Gamma^d{}_{ea}\,. \tag{1.13}$$

Since it could be confusing, from now on we are going to denote fourth dimension quantities with an upper left index (4), i.e., 4D-Riemann goes like ${}^{(4)}R_{abc}{}^d$.

Once defined the projected derivatives, the projected changes of normal vector are given by $\gamma_a^c\gamma_b^d\nabla_c n_d$. Thus, we can write out the extrinsic curvature tensor:

$$K_{ab} \equiv -\gamma_a^c\gamma_b^d\nabla_c n_d\,. \tag{1.14}$$

It is important to notice that, even though $\nabla_c n_d$ is not symmetric, the projection $D_a n_b$ is. This is because the normal vector is not the gradient of t, but related to it by α, (1.2). Thus, applying ∇_c on n_d doesn't generally commute, except for the cases where:

$$\nabla_{[a} n_{b]} = \frac{1}{2} \left(\nabla_b \alpha \nabla_a t - \nabla_a \alpha \nabla_b t \right) = 0 \,, \tag{1.15}$$

for example, $\alpha = \text{const} = 1$ (geodesic curves), allow us to commute $\nabla_c n_d$ since it lead us to $\nabla_c \nabla_d t = \nabla_d \nabla_c t$. The latter equality follows from the torsion free in ∇_c. However, once we project $\nabla_c n_d$ its antisymmetric part vanishes as follows:

$$\begin{aligned} K_{[ab]} &= \gamma_a^c \gamma_b^d \nabla_{[c} n_{d]} = \frac{1}{2} \gamma_a^c \gamma_b^d \left(\nabla_c n_d - \nabla_d n_c \right) \\ &= \frac{1}{2} \left[-\alpha \gamma_a^c \gamma_b^d \nabla_c \nabla_d t + \alpha \gamma_a^c \gamma_b^d \nabla_d \nabla_c t \right] \\ &= \frac{\alpha}{2} \gamma_a^c \gamma_b^d \left(\nabla_d \nabla_c t - \nabla_c \nabla_d t \right) = 0 \,. \end{aligned} \tag{1.16}$$

And therefore

$$K_{ab} = K_{(ab)} \,. \tag{1.17}$$

In figure (1.2), we can see that for different points of $\mathcal{T}$ the normal vector can have different values. Moreover, these changes in n^a are proportional to the extrinsic curvature as given by (1.14). But, in turn, n^a has information about $\mathcal{T}$ as being orthogonal to t-field's gradient. So, the latter means that K_{ab} is related to changes of $\mathcal{T}$ in the t-field. In order to obtain that relationship we use Lie's derivative along n^a.

1.2.1 Lie derivative

A Lie derivative is another way to calculate changes in tensorial objects. Perhaps, its main feature is that the changes are given along a vectorial flux.

The Lie derivative compares change in tensors in a limiting point, i.e., reaching it by a limit process. This comparison is made by being evaluated and dragged along a vector. Let's take a geometrical view of this. Figure (1.3) shows a tensor W_a^b changing in a vectorial flux $\vec{J}$ (gray arrows). Point A has associated x^c coordinates and B has $x^{c'}$. When W_a^b is evaluated in points $\{A, B\}$, its direction is thought to change. If we

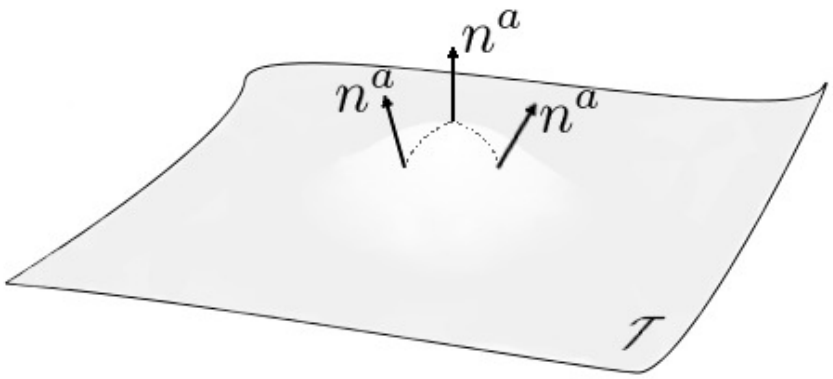

Figure 1.2: Because of bumps like the center one, n^a changes for different points at $\mathcal{T}$, these changes are proportional to extrinsic curvature.

were to compare $W_a^b(A)$ and $W_a^b(B)$ in A, we will end up with the partial derivative. On the other hand, if we drag W_a^b by parallel transport we get the covariant derivative. Instead, we want to drag the tensor by an infinitesimal change of coordinates, i.e., $x^{c'} = x^c + \delta\lambda J^c$ for some affine parameter λ. Then, with a change of coordinates, the dragged tensor is given by

$$W_{a'}^{b'}(B) = \frac{\partial x^{b'}}{\partial x^d}\frac{\partial x^c}{\partial x^{a'}} W_c^d(A)\,.$$

The comparison of this and $W_a^b(B)$ in A is taken to be the following limit:

$$\mathcal{L}_{\vec{J}} W_a^b \equiv \lim_{\delta\lambda\to 0} \frac{W_a^b(B) - W_{a'}^{b'}(B)}{\delta\lambda}\,.$$

This is the Lie derivative[BS10, Gou07]:

$$\mathcal{L}_{\vec{J}} W_a^b = J^c\partial_c W_a^b + W_c^b\partial_a J^c - W_a^c\partial_c J^b\,, \tag{1.18}$$

notice it has opposite signs to covariant derivative: negative for contraction on contravariant indices of the object, and positive for covariant ones. In spite of that, (1.18) has two remarkable differences from covariant derivative, it does not change the rank of the object and it does not depend on the connection coefficients.

In addition, since the procedure to construct (1.18) involves a change of coordinates, it allows to extend the Lie derivative for tensor densities. If S_a^b is a tensor density with

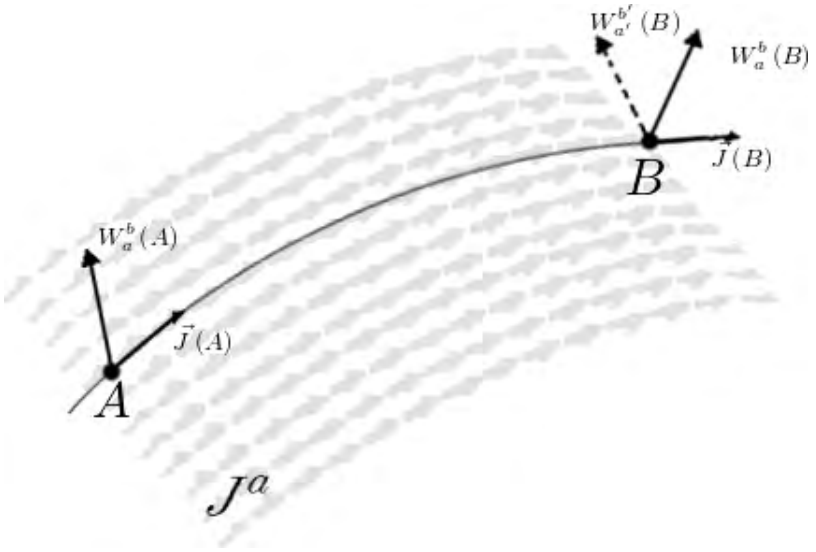

Figure 1.3: Change occurred in a tensor W^b_a along the vectorial flux $\vec{J}$.

weight $\mathcal{W}$, then its Lie derivative along $\vec{X}$ is given by [BS10, Alc08]:

$$\mathcal{L}_{\vec{X}} S^b_a = X^c \partial_c S^b_a + S^b_c \partial_a X^c - S^c_a \partial_c X^b + \mathcal{W} S^b_a \partial_c X^c \,. \tag{1.19}$$

Moreover, given that the connection coefficients are symmetric, the partial derivatives could be changed by the covariant ones:

$$\mathcal{L}_{\vec{J}} W^b_a = J^c \nabla_c W^b_a + W^b_c \nabla_a J^c - W^c_a \nabla_c J^b \tag{1.20}$$

$$\mathcal{L}_{\vec{X}} S^b_a = X^c \nabla_c S^b_a + S^b_c \nabla_a X^c - S^c_a \nabla_c X^b + \mathcal{W} S^b_a \nabla_c X^c \,. \tag{1.21}$$

From (1.21), it follows that the covariant derivative on tensor densities goes like:

$$\nabla_c S^b_a \equiv \partial_c S^b_a + \Gamma^b_{cd} S^d_a - \Gamma^d_{ca} S^b_d - \mathcal{W} S^b_a \Gamma^d_{dc} \,. \tag{1.22}$$

Notice that all derivatives (1.18)-(1.21) are linear operators. So, they posses the associative property and obey Leibnitz product rule.

Before we leave the section, we want to bring up one quick application for Lie Derivative. That is for Killing vectors. They represent spacetime symmetries.

Given a vector $\vec{\xi}$, we say it is a Killing vector if the metric tensor doesn't change for any value of it:

$$\mathcal{L}_{\vec{\xi}} g_{ab} = 0 \,. \tag{1.23}$$

So, from (1.18) and with $\nabla_c g_{ab} = 0$ we get the Killing equation:

$$\nabla_a \xi_b + \nabla_b \xi_a = 0\,. \tag{1.24}$$

It states that every Killing vector has an antisymmetric gradient. We reserve to obtain a Killing equation for tensor densities until chapter 2, where we actually use it.

1.2.2 Relation between γ_{ab} and K_{ab}

Once defined the Lie derivative, we are able to look for a relationship between the extrinsic curvature and the change of $\mathcal{T}$ in time. From (1.18) on the 3D-metric (1.6), we have:

$$\begin{aligned}
\mathcal{L}_{\vec{n}}\gamma_{ab} &= n^c\nabla_c\gamma_{ab} + \gamma_{ac}\nabla_b n^c + \gamma_{cb}\nabla_a n^c \\
&= n^c\nabla_c\left(n_a n_b\right) + \left(g_{ac} + n_a n_c\right)\nabla_b n^c + \left(g_{bc} + n_b n_c\right)\nabla_a n^c \\
&= n_a a_b + n_b a_a + \nabla_b n_a + \nabla_a n_b \\
&= 2n_{(a}a_{b)} + 2\nabla_{(a}n_{b)} \\
\frac{1}{2}\mathcal{L}_{\vec{n}}\gamma_{ab} &= n_{(a}a_{b)} + \nabla_{(a}n_{b)}\,.
\end{aligned} \tag{1.25}$$

Where we used the 4D-acceleration a_b, defined as [BS10]

$$a_b = n^a\nabla_a n_b\,. \tag{1.26}$$

It is useful to notice that a_b is spatial, i.e., it lies in $\mathcal{T}$. This is due to the fact that a level set's gradient is orthogonal to itself. Therefore, the gradient of n_b along itself is orthogonal to it, besides, given that n_b is orthogonal to $\mathcal{T}$, the result lies in the foliation $\mathcal{T}$.

On the other hand, the equation (1.25) also corresponds to the extrinsic curvature. To see it, let's use the projector γ_a^b in (1.14):

$$K_{ab} = -\left(\delta_a^c + n_a n^c\right)\left(\delta_b^d + n_b n^d\right)\nabla_c n_d\,,$$

where we may notice that terms with n^d yields to $n^d \nabla_c n_d$, which is zero. Thus, contracting the Deltas leads to:

$$K_{ab} = -\left(\nabla_a n_b + n_a n^c \nabla_c n_b\right) = -\left(\nabla_a n_b + n_a a_b\right) .$$

Finally, from (1.25) and since $K_{ab} = K_{(ab)}$ we get the relationship between K_{ab} and γ_{ab}:

$$K_{ab} = -\frac{1}{2}\mathcal{L}_{\vec{n}}\gamma_{ab} . \tag{1.27}$$

This equation shows how the extrinsic curvature measures the change in the 3D-metric along the global time t. This is a pretty geometric picture for K_{ab}, but we could say more about it. In particular, the trace of the extrinsic curvature has information about normal observers, i.e., observers along $\vec{n}$:

$$g^{ab}K_{ab} = K^a_a = K$$
$$K = -g^{ab}\left(\nabla_a n_b + n_a a_b\right) = -\nabla_b n^b - n^b a_b = -\nabla_b n^b ,$$

where we used that a_b is spatial. From [MTW73, Chp 10] we know that the four divergence of normal observers is related to their fractional change of proper volume, V_{ppr}:

$$\nabla_b n^b = \frac{1}{V_{\text{ppr}}}\left(\frac{d}{d\tau}V_{\text{ppr}}\right) ,$$

then

$$K = -\frac{1}{V_{\text{ppr}}}\frac{d}{d\tau}V_{\text{ppr}} . \tag{1.28}$$

As a result, if K has a high value, it would mean that the 3D-volume of normal observers is shrinking as fast as those $\mathcal{T}$ sheets are being carried along $\vec{n}$. At chapter 3, we will see that we could impose K to be zero, yielding to get rid of changes in coordinates at the time evolution of γ_{ab}.

In some sense, we have fulfilled the basic needs for Cauchy problem. Defining γ_{ab} will tell us about the structure of 3D-spacetime and once its related time derivative K_{ab} is defined too, we will know how $\mathcal{T}$ is changing in time.

1.3 Standard ADM equations

Now we can cast Einstein's equations to this 3+1 formulation, to do so we must develop relations between the Riemann tensor in $\mathcal{M}$ and its analogy at $\mathcal{T}$. A common prescription to do so, is reflected in what are collectively known as the Arnowitt, Deser and Misner (ADM) equations. Recalling we follow an established nomenclature in [BS10, Gou07], these quantities are labeled as ${}^{(4)}R_{abcd}$ and R_{abcd}, respectively. The latter is defined in a lookalike form to ${}^{(4)}R_{abcd}$:

$$R^{d}{}_{cba}w_d = 2D_{[a}D_{b]}w_c\,. \tag{1.29}$$

w_d is any spatial one-form. Following similar contractions on ${}^{(4)}R_{abcd}$, we have the 3D-Ricci tensor and scalar

$$R_{ab} = R^{c}{}_{acb} \tag{1.30a}$$

$$R = R^{a}_{a}\,. \tag{1.30b}$$

It is important to notice that these objects are purely spatial and only contain information about the curvature in $\mathcal{T}$ where they were created.

1.3.1 Gauss, Codazzi and Ricci equations

In order to reformulate the field equations, in this section we follow [BS10, Gou07]. To get the relationship between 4D and 3D Riemann tensors we will project ${}^{(4)}R_{abcd}$ with $\vec{n}$ and γ^{b}_{a}, at several and different orders to obtain the Gauss, Codazzi and Ricci equations. Those equations link the square of extrinsic curvature, and its spatial and time derivatives to the 4D-Riemann tensor. Then, we will use them with the field equations to develop a new set which takes advantage of the embedded spacetime that we are trying to use, $\mathcal{T}$.

Equation (1.29) can be expressed as

$$2D_{[a}D_{b]}V_c = 2\gamma_{ec}D_{[a}D_{b]}V^e = \gamma_{ec}R^{de}{}_{ba}V_d$$
$$D_aD_bV^e - D_bD_aV^e = R^{de}{}_{ba}V_d\,. \tag{1.31}$$

In order to develop this, we have to see what D_bV^e and $D_aD_bV^e$ are. From (1.9) the earlier is

$$D_bV^e = \gamma_b^p\gamma_q^e\nabla_pV^q = \gamma_b^p\left(g_q^e + n^en_q\right)\nabla_pV^q$$
$$= \gamma_b^p\nabla_pV^e + \gamma_b^pn^en_q\nabla_pV^q$$

and since $V^qn_q = 0$, it follows that $n_q\nabla_pV^q = -V^q\nabla_pn_q$. Then:

$$D_bV^e = \gamma_b^p\nabla_pV^e - \gamma_b^pn^eV^q\nabla_pn_q = \gamma_b^p\nabla_pV^e - n^eV^c\gamma_b^p\gamma_c^q\nabla_pn_q$$
$$= \gamma_b^p\nabla_pV^e + n^eV^cK_{bc}\,.$$

Thus, the first term of $R^{de}{}_{ba}V_d$ is:

$$D_aD_bV^c = \gamma_a^q\gamma_b^r\gamma_s^c\nabla_qD_rV^s = \gamma_a^q\gamma_b^r\gamma_s^c\nabla_q\left(\gamma_r^p\nabla_pV^s + n^sV^eK_{re}\right)$$
$$= \gamma_a^q\gamma_b^r\gamma_s^c\nabla_q\left[\left(g_r^p + n^pn_r\right)\nabla_pV^s + n^sV^eK_{re}\right]$$
$$= \gamma_a^q\gamma_b^r\gamma_s^c\nabla_q\nabla_rV^s + \gamma_a^q\gamma_b^r\gamma_s^c\nabla_q\left(n^pn_r\nabla_pV^s\right) + \gamma_a^q\gamma_b^r\gamma_s^c\nabla_q\left(n^sV^eK_{re}\right)\,. \tag{1.32}$$

In the last term, contributions carrying $\gamma_s^cn^s$ are zero since they are orthogonal, hence just one term remains

$$\gamma_a^q\gamma_b^r\gamma_s^cV^eK_{re}\nabla_qn^s = V^eK_{be}\gamma_a^q\gamma_s^c\nabla_qn^s\,.$$

From (1.14) $K^a{}_b = g^{aq}K_{qb} = -g^{aq}\gamma_q^r\gamma_b^s\nabla_sn_r = -\gamma^{ar}\gamma_b^s\nabla_sn_r$, therefore

$$\gamma_a^q\gamma_b^r\gamma_s^cV^eK_{re}\nabla_qn^s = K_{be}V^e\gamma_a^q\gamma_s^cg^{sf}\nabla_qn_f = -K_a^cK_{be}V^e\,.$$

In the second term of (1.32), contractions of $\gamma_b^rn_r$ are zero and we can put the rest in terms of K_{ab}:

$$\gamma_a^q\gamma_b^r\gamma_s^c\nabla_q\left(n^pn_r\nabla_pV^s\right) = \left(\nabla_pV^s\right)n^p\gamma_s^c\gamma_a^q\gamma_b^r\nabla_qn_r = -K_{ab}n^p\gamma_s^c\nabla_pV^s\,.$$

By putting these above expressions back into (1.32) we arrive at

$$D_a D_b V^c = \gamma_a^q \gamma_b^r \gamma_s^c \nabla_q \nabla_r V^s - K_{ab} \gamma_s^c n^p \nabla_p V^s - K_a^c K_{be} V^e. \tag{1.33}$$

Now, in (1.31) we got an interchange of a and b indices. From (1.33), we see its first term involves a and b in a contraction, so the indices who really matter are q and r. For the other terms the interchange is clear and (1.31) takes the form

$$R^{dc}{}_{ba} V_d = 2\gamma_a^q \gamma_b^r \gamma_s^c \nabla_{[q} \nabla_{r]} V^s - K_{[b}^c K_{a]e} V^e \,.$$

If we take down its index c; rename dummy indices $e \to d$, $s \to d$ and $d \to e$, and if we also notice that this equation stands for any spatial vector V^d, we arrive at the Gauss equation:

$$R_{abcd} + K_{ac} K_{bd} - K_{ad} K_{cb} = \gamma_a^p \gamma_b^q \gamma_c^r \gamma_d^{s\,(4)} R_{pqrs} \,. \tag{1.34}$$

It relates the 4D-Riemann tensor to its analogous in $\mathcal{T}$ and to a quadratic form of extrinsic curvature. Note that in (1.34) there are only projections with γ_a^b and none with $\vec{n}$.

The Codazzi equation is found by taking the covariant spatial derivative of K_{ab}:

$$\begin{aligned} D_a K_{bc} &= \gamma_q^p \gamma_b^q \gamma_c^r \nabla_p K_{qr} = -\gamma_q^p \gamma_b^q \gamma_c^r \left(\nabla_p \nabla_q n_r + \nabla_p (n_q a_r) \right) \\ &= -\gamma_q^p \gamma_b^q \gamma_c^r \nabla_p \nabla_q n_r + a_c K_{ab} \,. \end{aligned}$$

On the first row, we have again the contraction $\gamma_b^q n_q$, which makes the first term zero. Also, in the second row we used (1.26) and (1.14). Now, taking the anti-symmetric part on a and b indices, the second term vanishes since K_{ab} is symmetric. The remaining equation is what we were looking for

$$D_{[a} K_{b]c} = -\gamma_a^p \gamma_b^q \gamma_c^r \nabla_{[p} \nabla_{q]} n_r = \gamma_a^p \gamma_b^q \gamma_c^r n^{s\,(4)} R_{pqrs} \,. \tag{1.35}$$

Equation (1.35) has one projection with $\vec{n}$ and the rest with γ_a^b. Note that (1.34) and (1.35) only contain the spatial projector, extrinsic curvature and its spatial derivatives. This is a remarkable difference to the last equation, because it involves time derivatives of K_{ab}.

To take the next step on the way to reformulate Einstein's equations, let us develop the Lie derivative on K_{ab} along $\vec{n}$. First, expressing it as:

$$\begin{aligned}\mathcal{L}_{\vec{n}}K_{ab} &= n^c\nabla_c K_{ab} + K_{cb}\nabla_a n^c + K_{ac}\nabla_b n^c = n^c\nabla_c K_{ab} + K_{cb}\nabla_a n^c + K_{ca}\nabla_b n^c \\ &= n^c\nabla_c K_{ab} + 2K_{c(b}\nabla_{a)}n^c\,.\end{aligned}$$

but with $K_{cb} = -\left(\nabla_c n_b + n_c a_b\right)$ and its following variation

$$\nabla_c n_b = \nabla_c\left(g^{bd}g_{bd}n_b\right) = g_{bd}\nabla_c n^d \quad \Rightarrow \quad \nabla_c n^d = -g^{bd}K_{cb} - g^{bd}n_c a_b = -\left(K^d_c + n_c a^d\right)$$

or

$$\nabla_a n^c = -\left(K^c_a + n_a a^c\right)\,,$$

we have

$$\mathcal{L}_{\vec{n}}K_{ab} = -n^c\nabla_c\nabla_a n_b - n^c\nabla_c\left(n_a a_b\right) + 2K_{c(b}K^c_{a)} - 2K_{c(b}n_{a)}a^c \tag{1.36}$$

where we could rewrite the first term on the RHS with the aid of the 4D-Riemann tensor as:

$$n^c\nabla_c\nabla_a n_b = {}^{(4)}R_{dbac}n^d n^c + n^c\nabla_a\nabla_c n_b\,. \tag{1.37}$$

Before using this result, notice that its last term is related to $\nabla_a a_b = \nabla_a\left(n^c\nabla_c n_b\right)$. Taking its expansion and using the above expressions for $\nabla_a n^c$ and $\nabla_c n_b$, it follows that

$$\begin{aligned}\nabla_a a_b &= \left(K^c_a + n_a a^c\right)\left(K_{cb} + n_c a_b\right) + n^c\nabla_a\nabla_c n_b \\ &= K^c_a K_{cb} + n_c a_b K^c_a + n_a a^c K_{cb} + n_c a_b n_a a^c + n^c\nabla_a\nabla_c n_b\,,\end{aligned}$$

where the second and fourth terms are zero. Then, the relationship between $\nabla_a a_b$ and $n^c\nabla_a\nabla_c n_b$ is:

$$n^c\nabla_a\nabla_c n_b = \nabla_a a_b - K^c_a K_{cb} - n_a a^c K_{cb}\,.$$

With this equation in (1.37) and then in (1.36), the Lie derivative takes the form

$$\begin{aligned}\mathcal{L}_{\vec{n}}K_{ab} = -n^d n^{c\,(4)}R_{dbac} - \nabla_a a_b + K^c_a K_{cb} \;&+\; n_a a^c K_{cb} - n^c a_b\nabla_c n_a \\ &-\; n^c n_a\nabla_c a_b - 2K^c_{(a}K_{b)c} - 2K_{c(a}n_{b)}a^c\,.\end{aligned}$$

The third and fourth terms of this equation cancel out one part of those symmetric terms. Also, from [BS10, Gou07], we know that the Lie derivative applied on spatial tensors leaves them spatial when it's along $\vec{n}$. Thus, we could project those free indices in the above equation with $\gamma_a^q \gamma_b^r$. This will leave it unchanged ($\gamma_a^q \gamma_b^r \mathcal{L}_{\vec{n}} K_{ab} = \mathcal{L}_{\vec{n}} K_{ab}$). Then, rewriting the $D_a a_b + a_a a_b$ terms in the last equation with the following expression,

$$\begin{aligned} D_a a_b = D_a \left(D_b \ln \alpha\right) &= D_a \left(\frac{1}{\alpha} D_b \alpha\right) + \frac{1}{\alpha} D_a D_b \alpha \\ &= \frac{1}{\alpha} D_a D_b \alpha - \alpha^{-2} \left(D_a \alpha\right) \left(D_b \alpha\right) = \frac{1}{\alpha} D_a D_b \alpha - a_a a_b \\ \frac{1}{\alpha} D_a D_b \alpha &= D_a a_b + a_a a_b \,, \end{aligned} \tag{1.38}$$

thus, we arrive at an expression for the change of extrinsic curvature along $\vec{n}$, which is known as the Ricci equation:

$$\mathcal{L}_{\vec{n}} K_{ab} = -n^d n^c \gamma_a^q \gamma_b^{r\,(4)} R_{drqc} - \frac{1}{\alpha} D_a D_b \alpha - K_b^c K_{ac} \,. \tag{1.39}$$

Note that (1.39) contains two spatial and two time projections, it also contains the lapse function, α, meaning that this equation will be involved in the evolution of $\mathcal{T}$.

1.3.2 Constraint equations

Now we already have Gauss, Codazzi and Ricci equations, let's get the constraint equation, which we sighted at section 1.1. In order to do so, let's define the energy and momentum densities as:

$$\rho \equiv n_a n_b T^{ab} \tag{1.40a}$$

$$S_a \equiv -\gamma_a^b n^c T_{bc} \,. \tag{1.40b}$$

Because of the projection with the normal vector, these objects are seen from normal observers. On the other hand, we can use (1.40a) and (1.40b) with Einstein's equations

$$G^{ab} = 8\pi T^{ab} \,, \tag{1.41}$$

to see the matter aspects in (1.34) and (1.35). From (1.41) we have the following equation for (1.40a)

$$\begin{aligned} 8\pi\rho = G_{ab}n^a n^b &= {}^{(4)}R_{ab}n^a n^b - \frac{1}{2}n^a n^b g_{ab}{}^{(4)}R \\ 16\pi\rho &= 2{}^{(4)}R_{ab}n^a n^b - n^a n^b\left(\gamma_{ab} - n_a n_b\right){}^{(4)}R \\ &= 2{}^{(4)}R_{ab}n^a n^b + {}^{(4)}R\,. \end{aligned} \tag{1.42}$$

And this equation is the double contraction of Gauss equation, from (1.34) we have that

$$\gamma^p_a\gamma^q_b\gamma^r_c\gamma^{s(4)}_d R_{pqrs} = g_{aa'}\gamma^{a'p}g_{bb'}\gamma^{b'q}\gamma^r_c\gamma^{s(4)}_d R_{pqrs}\,.$$

Then, contracting a' with c and b' with d leads to

$$g_{ac}g_{bd}\gamma^{pr}\gamma^{qs(4)}R_{pqrs}\,.$$

And using (1.6) with the symmetries of the 4D-Riemann tensor [BS10, Sec 2.5] it becomes

$$n^r n^p n^{q(4)}R_{pqrs} = 0\,. \tag{1.43}$$

Where the expansion of $\gamma^{pr}\gamma^{qs(4)}R_{pqrs}$ exactly leads to the RHS of (1.42). On the other hand, this equation is:

$$\gamma^{pr}\gamma^{qs(4)}R_{pqrs} = g^{ac}g^{bd}\left(R_{abcd} + K_{ac}K_{bd} - K_{ad}K_{cb}\right) = R + K - K^{cb}K_{cb}\,,$$

then, together with (1.42) it gives the Hamiltonian constraint equation:

$$R + K^2 - K^{ab}K_{ab} = 16\pi\rho\,. \tag{1.44}$$

It's worth to notice that, equation (1.44) keeps one of the essences of GR, we mean, the presence of matter disturbs the surrounding spacetime by means of curvature, and in vice-versa. In fact, (1.44) is very relevant in the chapter 3 of this work.

Similar to the previous procedure, using (1.40b) along with (1.41) leads to another constraint equation, $8\pi S_a = -\gamma^b_a n^c G_{bc}$, where

$$\begin{aligned} -\gamma^b_a n^c G_{bc} &= -\gamma^b_a n^c\left[{}^{(4)}R_{bc} - \frac{1}{2}g_{bc}{}^{(4)}R\right] = -\gamma^b_a n^{c(4)}R_{bc} + \frac{1}{2}g_{bc}\gamma^b_a n^{c(4)}R \\ &= -\gamma^b_a n^{c(4)}R_{bc}\,, \end{aligned} \tag{1.45}$$

Where, the RHS of (1.45) can be expressed in terms of Codazzi's equation. In order to do so, we take a contraction on indices a and c of (1.35). We can make this by multiplying (1.35) by $g^{aa'}g_{qa'} = \delta^a_q$. Then, performing the contraction of a' and c indices leads to:

$$g_{aa'}\gamma^{a'p}\gamma^q_b\gamma^r_c n^{s(4)}R_{pqrs} \quad \longrightarrow \quad g_{ac}\gamma^{cp}\gamma^r_c\gamma^q_b n^{s(4)}R_{pqrs} = \gamma^{rp}\gamma^q_b n^{s(4)}R_{pqrs}\,,$$

hence,

$$\begin{aligned} g^{ac}D_{[a}K_{b]c} &= \gamma^{rp}\gamma^q_b n^{s(4)}R_{pqrs} = n^s\gamma^{q(4)}_b R_{qs} + n^s\gamma^q_b n^p n^{r(4)}R_{pqrs} \\ g^{ac}D_{[a}K_{b]c} &= \gamma^q_b n^{s(4)}R_{qs}\,. \end{aligned}$$

We have used (1.6) and (1.43) in order to get the last row. Finally, introducing this expression in (1.45) we get the momentum constraint equation

$$g^{ac}D_{[a}K_{b]c} = D_aK^a_b - D_bK = 8\pi S_b\,. \tag{1.46}$$

The relation between flux of matter and changes in the curvature. However, remember that now, we are in 3D and the changes are in the extrinsic curvature as seen from normal observers. Plus, those changes in K_{ab} are given momentarily in the global time t, where $\mathcal{T}$ resides.

Now, let's get the equation that tells how the changes of γ_{ab} and K_{ab} are threading in time.

1.3.3 Evolution equations

The arbitrary choice we made in section 1.1 of t, as the global parameter for ordering the $\mathcal{T}$ spaces, carries some consequences. The most relevant, is that our most close common observers, normal observers $\vec{n}$, are not the right choices to develop the constraint equations. This is because they are not dual to $\nabla_a t$. As we made $\vec{n}$ to be unitary and hence, left out this duality, i.e., the RHS of

$$n^a\nabla_a t = \alpha^{-1}\,, \tag{1.47}$$

is in general different from one. However, is fixed by introducing a new vector dual to t:

$$\vec{t} = \alpha\vec{n} + \vec{\beta}\,, \tag{1.48}$$

where $\vec{\beta}$ is purely spatial. From (1.2) the time vector $\vec{t}$ is dual to the global time, $t^a\nabla_a t = 1$. If we use (1.48) to evolve $\mathcal{T}$, we are left with another choice to make on $\vec{\beta}$. The meaning of $\vec{\beta}$ is clearer when we take $\alpha = 1$, then the difference between $\vec{t}$ and $\vec{n}$ is purely spatial, because of that $\vec{\beta}$ is called the shift vector, and it plays the active role of translating or rotating the spatial coordinates from one spatial sheet to the next while they are being evolved along $\vec{t}$.

The change of the 3D-metric along $\vec{t}$ could be calculated from its relation with extrinsic curvature (1.27)

$$\alpha K_{ab} = -\frac{1}{2}\alpha\mathcal{L}_{\vec{n}}\gamma_{ab}\,,$$

then, the Lie derivative of γ along $\vec{t}$ is:

$$\mathcal{L}_{\vec{t}}\gamma_{ab} = \alpha\mathcal{L}_{\vec{n}}\gamma_{ab} + \mathcal{L}_{\vec{\beta}}\gamma_{ab} = -2\alpha K_{ab} + \mathcal{L}_{\vec{\beta}}\gamma_{ab}\,, \tag{1.49}$$

where the derivative operator along $\vec{t}$ is separated in two terms, we see below, that when we take a Lie derivative on a spatial object and it is along a time-like vector it could be separated like we did in (1.49). We already had this kind of relationship between the 3D-metric and extrinsic curvature, but now in (1.49) the lapse function is explicit. Also we have found that γ_{ab} changes along $\vec{\beta}$. In the next chapter we discuss some popular selections for those quantities, for now let's move on to the last of the ADM equations.

The changes of K_{ab} in time are calculated with the Lie derivative along the time vector:

$$\begin{aligned}\mathcal{L}_{\vec{t}}K_{ab} &= t^c\nabla_c K_{ab} + 2K_{c(a}\nabla_{b)}t^c \\ &= \alpha n^c\nabla_c K_{ab} + \beta^c\nabla_c K_{ab} + 2K_{c(a}\nabla_{b)}\left(\alpha n^c + \beta^c\right)\,,\end{aligned} \tag{1.50}$$

and keeping in mind that

$$\mathcal{L}_{\vec{n}} K_{ab} = n^c \nabla_c K_{ab} + 2K_{c(a}\nabla_{b)} n^c \,,$$

(similar for the shift vector), we can expand (1.50) as two Lie derivatives, one along $\alpha\vec{n}$ and the other in $\vec{\beta}$

$$\mathcal{L}_{\vec{t}} K_{ab} = \alpha n^c \nabla_c K_{ab} + 2\left[n^c K_{c(a}\nabla_{b)}\alpha + \alpha K_{c(a}\nabla_{b)} n^c\right] + \beta^c \nabla_c K_{ab} + 2K_{c(a}\nabla_{b)}\beta^c \,.$$

The first term in squared parenthesis is zero since n^c and K_{ca} are orthogonal to each other, then

$$\begin{aligned}\mathcal{L}_{\vec{t}} K_{ab} &= \alpha\left[n^c \nabla_c K_{ab} + 2K_{c(a}\nabla_{b)} n^c\right] + \beta^c \nabla_c K_{ab} + 2K_{c(a}\nabla_{b)}\beta^c \\ &= \alpha \mathcal{L}_{\vec{n}} K_{ab} + \mathcal{L}_{\vec{\beta}} K_{ab} \,. \end{aligned} \tag{1.51}$$

As we see, any factor multiplied by the normal vector is taken outside of the derivative when it acts on any spatial object. Also any vector being added to $\vec{n}$ yields to another derivative term. We made use of these features in (1.49).

We can't go further on the second term of (1.51) until we choose $\vec{\beta}$. However, we already have information about the other term, therefore, using (1.39) we rewrite (1.51).

First of all, introducing the 3D-metric, 1.6, the RHS of (1.51) can be divided as follows:

$$\begin{aligned} n^d n^c \gamma_a^q \gamma_b^{r\,(4)} R_{drcq} &= \left(\gamma^{dc} - g^{dc}\right)\gamma_a^q \gamma_b^{r\,(4)} R_{drcq} = \gamma^{dc}\gamma_a^q \gamma_b^{r\,(4)} R_{drcq} - \gamma_a^q \gamma_b^{r\,(4)} R_{rq} \\ &= R_{ab} + K K_{ab} - K_b^c K_{ca} - 8\pi \gamma_a^q \gamma_b^r \left(T_{qr} - \frac{1}{2} g_{qr} T\right) \,, \end{aligned}$$

where we used a contraction of the Gauss equation (1.34) in the fisrt term and ${}^{(4)}R_{ab} = 8\pi\left(T_{ab} - \frac{1}{2}g_{ab}T\right)$ in the second. In addition, defining the spatial stress tensor as:

$$S_{ab} \equiv \gamma_a^c \gamma_b^d T_{cd} \tag{1.52}$$

and its trace

$$S \equiv S_a^a \,, \tag{1.53}$$

we can rewrite the last term in Ricci equation as:

$$\begin{aligned}8\pi\gamma_b^a\left(T_{ab}-\frac{1}{2}g_{ab}T\right) &= 8\pi S_{ab}-4\pi\gamma_a^q\gamma_b^r g_{qr}g^{dc}T_{dc}\\ &= 8\pi S_{ab}-4\pi\gamma_{ab}\left(\gamma^{dc}-n^d n^c\right)T_{dc} = 8\pi S_{ab}+4\pi\rho\gamma_{ab}-4\pi\gamma_{ab}\gamma^{dc}T_{dc}\\ &= 8\pi S_{ab}+4\pi\gamma_{ab}\left(\rho-S\right)\,,\end{aligned}$$

where we used $S_a^b = g^{bf}\gamma_a^q\gamma_f^r T_{qr} = \gamma_a^q\gamma^{rb}T_{qr}$. So, the Ricci equation can be expressed as

$$\begin{aligned}\mathcal{L}_{\vec{n}}K_{ab} &= R_{ab}+KK_{ab}-K_b^cK_{ca}-8\pi\left[S_{ab}+\frac{1}{2}\gamma_{ab}\left(\rho-S\right)\right]-\frac{1}{\alpha}D_aD_b\alpha-K_b^cK_{ca}\\ \alpha\mathcal{L}_{\vec{n}}K_{ab} &= \alpha\left(R_{ab}+KK_{ab}-2K_b^cK_{ca}\right)+8\pi\alpha\left[\frac{1}{2}\gamma_{ab}\left(\rho-S\right)-S_{ab}\right]-D_aD_b\alpha\,.\end{aligned}$$

This equation implies that, temporal changes in K_{ab} follow the next expression:

$$\mathcal{L}_{\vec{t}}K_{ab} = \alpha\left(R_{ab}+KK_{ab}-2K_b^cK_{ca}\right)+8\pi\alpha\left[\frac{1}{2}\gamma_{ab}\left(\rho-S\right)-S_{ab}\right]-D_aD_b\alpha+\mathcal{L}_{\vec{\beta}}K_{ab}\,, \tag{1.54}$$

as we see, this is an evolution equation for the extrinsic curvature.

The complete set of ADM equations provides a whole reformulation of Einstein's equations. The momentum and hamiltonian constraint equations give the needed conditions to define each spatial geometry, while the evolution equations thread them in time.

In order to make the ADM equations simpler we use a coordinate basis system, $\left\{\vec{e}_{(0)},\vec{e}_{(1)},\vec{e}_{(2)},\vec{e}_{(3)}\right\}$. Due to evolution equations, a natural choice is to define one of our basis along the time vector

$$\vec{e}_{(0)} = \vec{t}\equiv(1,0,0,0) \tag{1.55}$$

and the rest on the foliations, i.e., they are spatial vectors

$$\vec{e}_{(1)}\cdot\vec{n} = \vec{e}_{(2)}\cdot\vec{n} = \vec{e}_{(3)}\cdot\vec{n} = 0\,. \tag{1.56}$$

From its definition, the Lie derivative along $\vec{t}$ is reduced to partials ∂_t. Moreover, since $\vec{e}_{(i)}$ can not be zeros, from (1.56) the i-components of n_a must be zeroes

$$n_i = 0\,, \tag{1.57}$$

which means that for any spatial vector, its 0-index component (contravariant) is zero. For example, the shift vector

$$\beta^a = \left(0, \beta^i\right) \ . \tag{1.58}$$

This is a remarkable thing, now we know that all the spatial objects have their whole information in spatial indices. This is clear in contravariant indices for the above equation, but it is also true for the covariant ones [BS10]. In addition to (1.58), if we use the definitions for $\vec{t}$ and γ_{ab}, as given in (1.48) and (1.6), respectively. We get the following results:

$$n^a = \left(\alpha^{-1}, -\alpha^{-1}\beta^i\right) \tag{1.59a}$$

$$n_a = \left(\alpha^{-1}, 0, 0, 0\right) \tag{1.59b}$$

$$\gamma_{ij} = g_{ij} \tag{1.59c}$$

$$g_{ab} = \begin{pmatrix} -\alpha^2 + \beta^k\beta_k & \beta_i \\ \beta_j & \gamma_{ij} \end{pmatrix} \ . \tag{1.59d}$$

They all are useful equations but we will focus on (1.59c) for now. This equation relates the covariant components of each metric, but since for spatial objects we could disregard the zero index, it also stands that it is possible to use γ_{ij} for lowering the spatial indices in any tensor object. This is important because we can rewrite the set of ADM equations in an easier way.

The constraint equations contain the extrinsic curvature, dropping its 0-indices, they are rewritten as

$$R + K^2 + K_{ij}K^{ij} = 16\pi\rho \tag{1.60a}$$

$$D_j K^j_i - D_i K = 8\pi S_i \, . \tag{1.60b}$$

A very similar thing can be done with the evolution equations: terms involving the Lie derivative along $\vec{\beta}$ can be expressed in a more convenient form. First, let's see what $\mathcal{L}_{\vec{\beta}}\gamma_{ij}$ is:

$$\mathcal{L}_{\vec{\beta}}\gamma_{ij} = \beta^k\nabla_k\gamma_{ij} + 2\gamma_{k(i}\nabla_{j)}\beta^k \, ,$$

from (1.59c) we have $\nabla_j = g^k_j \nabla_k = \gamma^k_j \nabla_k$, then the first term vanishes and the second one is:

$$\begin{aligned} 2\gamma_{l(i}\nabla_{j)}\beta^l &= \gamma_{li}\nabla_j\beta^l + \gamma_{lj}\nabla_i\beta^l = \gamma_{li}\gamma^k_j\nabla_k\beta^l + \gamma_{lj}\gamma^k_i\nabla_k\beta^l \\ &= g_{mi}\gamma^m_l\gamma^k_j\nabla_k\beta^l + g_{mj}\gamma^m_l\gamma^k_i\nabla_k\beta^l \\ &= g_{mi}D_j\beta^m + g_{mj}D_i\beta^m = D_j\beta_i + D_i\beta_j\,, \end{aligned}$$

where we used $D_a g_{bc} = 0$. It follows from the projected covariant derivative, D_a, (1.9). Therefore,

$$\mathcal{L}_{\vec{\beta}}\gamma_{ij} = 2D_{(i}\beta_{j)}\,.$$

In a similar way the Lie derivative along $\vec{\beta}$ in the evolution equation for K_{ij} can be expressed as:

$$\mathcal{L}_{\vec{\beta}}K_{ij} = \beta^k D_k K_{ij} + 2K_{k(i}D_{j)}\beta^k,$$

hence, the ADM evolution equations get the following form:

$$\partial_t\gamma_{ij} = -2\alpha K_{ij} + D_i\beta_j + D_j\beta_i \tag{1.61a}$$

$$\begin{aligned} \partial_t K_{ij} = &-D_iD_j\alpha + \alpha\left(R_{ij} - 2K_{il}K^l_j + KK_{ij}\right) - 8\pi\alpha\left[S_{ij} - \frac{1}{2}\gamma_{ij}\left(S-\rho\right)\right] \\ &+ \beta^k D_k K_{ij} + K_{kj}D_i\beta^k + K_{ik}D_j\beta^k\,. \end{aligned} \tag{1.61b}$$

In comparison to (1.49) and (1.54) these equations look more solvable since now we have an idea how to operate on $\vec{\beta}$. Notice that lapse function and shift vector are only in the evolution equations, this makes sense since those gauges will lead us to evolve the obtained solutions from (1.60a) and (1.60b). While α and $\vec{\beta}$ can be included implicitly in the ADM equations, it has been proved [SY78] that an explicit way helps in the evolving process making it more stable. In addition, a well made choice for $\vec{\beta}$, allows to control numerical developments for intrinsic rotating spacetimes, like the Kerr solution to Einstein's equations or a binary neutron stars system.

Chapter 2

CTT formalism and Gauge conditions

The ADM equations have some similarities to Maxwell's equations in electromagnetic theory. In a flat spacetime, the electromagnetic field equations are:

$$D_i E^i = 4\pi\rho \tag{2.1a}$$

$$D_i B^i = 0 \tag{2.1b}$$

$$\partial_t A_i = -E_i - D_i\phi \tag{2.1c}$$

$$\partial_t E_i = D_i D^j A_j - D^j D_j A_i - 4\pi j\,, \tag{2.1d}$$

where $A^a = (\phi, A^i)$ is the vector potential and is related to the magnetic field by $B_i = \epsilon_{ijk} D^j A^k$ with ϵ_{ijk} being the Levi-Civitta symbol. Now, by identifying, A_i with γ_{ij} and E_i with K_{ij} we notice the similarity. The RHS of the evolution equations for $\{A_i, \gamma_{ij}\}$ have a field variable and a spatial derivative of a gauge variable while those for $\{E_i, K_{ij}\}$ involve matter source terms and second spatial derivatives of field variables. On the constrictions side we have constraints in divergences of the electric field and extrinsic curvature.

This motivates us to seek for a solution in a similar way as that the employed in electromagnetic theory. The coupled system (2.1a)-(2.1d) is usually molded to find the electromagnetic wave equations. In order to solve the resulting equations it is common to decompose the field variables in their transverse and longitudinal parts to make use of symmetries[Gre98, Chp 15].

In spite of the similarities between (2.1a)-(2.1d) and (1.60a)-(1.61b), the most remarkable difference is that the latter system is not linear in field variables, $\{\gamma_{ij}, K_{ij}\}$. With the aim of rewriting the ADM equations in a more suggestive structure, we may

classify the constraint equations as a system of coupled elliptical equations. However, (1.61a) and (1.61b) will not have definitive forms until we choose the information about gauges α and $\vec{\beta}$. In spite of this, efforts of York and others [MTW73, Sec.21.11] to introduce some decomposition for field variables have been giving fantastic results, many of them are contemporary works on the subject.

2.1 CTT decomposition

There are two ways to proceed in such decomposition. One is using some conformal mapping of the field variables. The other one using the objects by themselves. These are called Conformal Transverse Trace-less (CTT) and Physical Transverse Trace-less (PTT) decomposition, respectively. We use the first one, not only because our main goal requires it, but also allows us to improve the numerical process [Alc08, Cho07, Lag04].

In CTT formalism, the 3D-metric γ_{ij} has the following conformal mapping [BS10]:

$$\gamma_{ij} \equiv \psi^4 \bar{\gamma}_{ij} \tag{2.2a}$$

$$\bar{\gamma}_{ij} \equiv \gamma^{-\frac{1}{3}} \gamma_{ij} \,, \tag{2.2b}$$

where ψ is the conformal factor. The second definition is chosen in such way that the $\bar{\gamma}_{ij}$'s determinant is 1. From both definitions we note that conformal factor is related to the γ_{ij}'s determinant by:

$$\gamma = \psi^{12} \,. \tag{2.3}$$

Indeed, if we consider the mapping (2.2b) as a linear transformation, the factor $\gamma^{\frac{\mathcal{W}}{2}}$ leads us to think of $\bar{\gamma}_{ij}$ as a tensor density with weight $\mathcal{W}$, [Alc08, P.85]. Therefore, the conformal 3D-metric is a tensor density with weight of $-\frac{2}{3}$. From now on, we refer to $\bar{\gamma}_{ij}$ as the conformal metric, since we are not going to use some $\bar{g}_{ij}$ or any fourth dimension conformal object.

Conformal mapping has been used in other physical theories; for example it is used to drop off any global parameter which is expected to be a degree of freedom. Generally, it eases the problem, e.g., stereographic projection is a conformal mapping which helps to handle regions at infinity [BY80]. Keeping in mind that conformal mapping would simplify our equation system, we could imagine that everyone might want to push their own theories to this ground. Sadly, not every theory is viable for a conformal approach. The main requirement is that the equations should be conformally invariant [Wal84]. In spite of this, the ADM equations are conformally invariant and the above examples are what we gain in CTT [MTW73, Alc08, BS10].

On the other hand, the fact that $\nabla_a g_{bc} = 0$ means that the covariant derivative ∇_a is attached to the spacetime metric, however, if we had another metric, say the conformal one, it would not commute with ∇_a. However, there should be another covariant derivative which is attached to $\bar{\gamma}_{bc}$, say a conformal covariant derivative, $\bar{\nabla}_a$. The relationship between these two operators is given by [Wal84]:

$$\bar{\nabla}_a w_b = \nabla_a w_b - w_c C^c{}_{ab} \tag{2.4a}$$

$$\bar{\nabla}_a w^b = \nabla_a w^b - w^c C^b{}_{ac}\,, \tag{2.4b}$$

where $\{w_c, w^c\}$ are any one-form and vector given. Once we attach one covariant derivative, namely $\bar{D}_j$, to $\bar{\gamma}_{ij}$, those coefficients $C^c{}_{ab}$ in (2.4a-2.4b) take the form [Wal84]

$$C^i{}_{jk} = \frac{1}{2}\bar{\gamma}^{il}\left(D_j\bar{\gamma}_{kl} + D_k\bar{\gamma}_{jl} - D_l\bar{\gamma}_{jk}\right)\,. \tag{2.5}$$

In equation (1.10) D_a is attached to γ_{bc}, therefore we can express $D_i\bar{\gamma}_{jk}$ as:

$$D_i\bar{\gamma}_{jk} = \psi^4 D_i\left(\psi^{-4}\bar{\gamma}_{jk}\right) + 4\bar{\gamma_{jk}}D_i\ln\psi\,.$$

Using this in (2.5), we arrive to the relationship between $\bar{D}_j$ and D_j:

$$C^i{}_{jk} = 2\left[2\delta^i{}_{(k}D_{j)}\ln\psi - \bar{\gamma}^{il}\bar{\gamma}_{jk}D_l\ln\psi\right]\,. \tag{2.6}$$

In a similar way, once the attachment of $\bar{D}_i\bar{\gamma}_{jk} = 0$ is made, the above coefficients could be expressed in terms of $\bar{D}_j$ and γ_{ij}. These are:

$$C^i{}_{jk} = 2\left[2\delta^i{}_{(k}\bar{D}_{j)}\ln\psi - \gamma^{il}\gamma_{jk}\bar{D}_l\ln\psi\right] . \tag{2.7}$$

Since $C^i{}_{jk}$ are defined in terms of $\bar{\gamma}_{jk}$ they inherit its symmetry. Notice that replacing D_j and $\bar{\gamma}_{ij}$ in (2.5) by ∂_j and γ_{ij} we recover the Christoffel symbols. Just as $C^i{}_{jk}$ relates $\bar{D}_j$ to D_j, those symbols relate partial to covariants derivatives.

In order to obtain a set of equations in CTT we begin by splitting up the extrinsic curvature in its trace and trace-less parts

$$K_{ij} = A_{ij} + \frac{1}{3}K\gamma_{ij} . \tag{2.8}$$

The conformal expressions for A_{ij}, which is the trace-less part, and K are chosen to be

$$A^{ij} = \psi^{-10}\bar{A}^{ij} \tag{2.9a}$$

$$K = \bar{K} . \tag{2.9b}$$

Thus implying that

$$A_{ij} = \psi^{-2}\bar{A}_{ij} \tag{2.10}$$

and

$$D_jA^{ij} = \psi^{-10}\bar{D}_jA^{ij} . \tag{2.11}$$

From (2.8) we got that

$$\begin{aligned} K_{ij}K^{ij} &= \left(\psi^{-2}\bar{A}_{ij} + \frac{1}{3}\bar{\gamma}_{ij}\psi^4K\right)\left(\psi^{-10}\bar{A}^{ij} + \frac{1}{3}\psi^{-4}\bar{\gamma}^{ij}K\right) \\ &= \psi^{-12}\bar{A}_{ij}\bar{A}^{ij} + \frac{\delta^i_i}{9}K^2 + \frac{1}{3}\psi^{-6}\bar{A}^{ij}\bar{\gamma}_{ij}K + \frac{1}{3}\psi^{-6}\bar{A}_{ij}\bar{\gamma}^{ij}K \\ &= \psi^{-12}\bar{A}_{ij}\bar{A}^{ij} + \frac{1}{3}K^2 \end{aligned}$$

since $\delta^i_i = 3$ and $\bar{A}_{ij}\bar{\gamma}^{ij} = \bar{A}^{ij}\bar{\gamma}_{ij} = \bar{A}^i_i = 0$.

Then, to transform the ADM equations we need the conformal Ricci tensor, $\bar{R}_{ij}$, and its contraction given by [BS10]:

$$\begin{aligned} R_{ij} = \bar{R}_{ij} &- 2\left(\bar{D}_i\bar{D}_j \ln\psi + \bar{\gamma}_{ij}\bar{\gamma}^{lm}\bar{D}_l\bar{D}_m \ln\psi\right) \\ &+ 4\left(\left(\bar{D}_i \ln\psi\right)\left(\bar{D}_j \ln\psi\right) - \bar{\gamma}_{ij}\bar{\gamma}^{lm}\left(\bar{D}_i \ln\psi\right)\left(\bar{D}_j \ln\psi\right)\right) \qquad (2.12a) \\ R = \psi^{-4}\bar{R} &- 8\psi^{-5}\bar{D}^2\psi\,, \qquad (2.12b) \end{aligned}$$

with short hand for the operator $\bar{D}^2 = \bar{\gamma}^{ij}\bar{D}_i\bar{D}_j$. Inserting the equation (2.12b) and the above expression for $K_{ij}K^{ij}$ into (1.60a) will lead us to the conformal equation for the hamiltonian constraint

$$\psi\bar{R} + 8\bar{D}^2\psi + \psi^{-7}\bar{A}_{ij}\bar{A}^{ij} - \frac{2}{3}K^2 = 16\pi\rho\psi^5\,. \qquad (2.13)$$

However, to transform the momentum constraint we need to express the covariant derivative D_j in terms of $\bar{D}_j$. First, using (2.8) into (1.60b) we have

$$\begin{aligned} 8\pi S^i =& D_j\left(\psi^{-10}\bar{A}^{ij} - \frac{2}{3}\psi^{-4}\bar{\gamma}^{ij}K\right) \\ =& D_j\left(\psi^{-10}\bar{A}^{ij}\right) + D_j\left(-\frac{2}{3}\psi^{-4}\bar{\gamma}^{ij}K\right)\,. \qquad (2.14) \end{aligned}$$

The first term, from (2.4b), becomes

$$D_j\left(\psi^{-10}\bar{A}^{ij}\right) = \bar{D}_j\left(\psi^{-10}\bar{A}^{ij}\right) + \psi^{-10}\bar{A}^{lj}C^i{}_{lj} + \psi^{-10}\bar{A}^{il}C^j{}_{jl}\,, \qquad (2.15)$$

where it follows that

$$\bar{D}_j\left(\psi^{-10}\bar{A}^{ij}\right) = \psi^{-10}\bar{D}_j\bar{A}^{ij} - 10\psi^{-10}\bar{A}^{ij}\bar{D}_j \ln\psi\,. \qquad (2.16a)$$

For the last terms of (2.15) we use (2.7) and $\gamma_{ij}\gamma^{kl} = \left(\psi^4\bar{\gamma}_{ij}\right)\left(\psi^{-4}\bar{\gamma}^{kl}\right) = \bar{\gamma}_{ij}\bar{\gamma}^{kl}$; hence

$$\begin{aligned} \bar{A}^{lj}C^i{}_{lj} &= 2\bar{A}^{lj}\left(2\delta^i{}_{(l}\bar{D}_{j)} \ln\psi - \bar{\gamma}_{lj}\bar{\gamma}^{ik}\bar{D}_k \ln\psi\right) = 2\left(\bar{A}^{ij}\bar{D}_j \ln\psi + \bar{A}^{il}\bar{D}_l \ln\psi\right) \\ &= 4\bar{A}^{il}\bar{D}_l \ln\psi \qquad (2.16b) \\ \bar{A}^{il}C^j{}_{lj} &= 2\bar{A}^{il}\left(2\delta^j{}_{(j}\bar{D}_{l)} \ln\psi - \bar{\gamma}_{lj}\bar{\gamma}^{jk}\bar{D}_k \ln\psi\right) = 2\left[\bar{A}^{il}\left(3\bar{\gamma}^{il}\bar{D}_l \ln\psi + \bar{\gamma}^{ij}\bar{D}_j \ln\psi\right) + \bar{A}^{ik}\bar{D}_k \ln\psi\right] \\ &= 6\bar{A}^{il}\bar{D}_l \ln\psi\,. \qquad (2.16c) \end{aligned}$$

The second term of (2.14) is developed in a similar way to the first term

$$D_j\left(-\frac{2}{3}\psi^{-4}K\bar{\gamma}^{ij}\right)=-\frac{2}{3}\left[\bar{D}_j\left(\psi^{-4}K\bar{\gamma}^{ij}\right)+\psi^{-4}K\bar{\gamma}^{lj}C^{i}{}_{jl}+\psi^{-4}K\bar{\gamma}^{ij}C^{j}{}_{jl}\right]$$

where

$$\bar{D}_j\left(\psi^{-4}K\bar{\gamma}^{ij}\right)=\bar{\gamma}^{ij}\psi^{-4}\bar{D}_jK-4K\psi^{-4}\bar{\gamma}^{ij}\bar{D}_j\ln\psi \tag{2.17a}$$

$$\begin{aligned}\psi^{-4}K\bar{\gamma}^{lj}C^{i}{}_{jl}&=2K\psi^{-4}\bar{\gamma}^{lj}\left(2\delta^{i}{}_{(j}\bar{D}_{l)}\ln\psi-\bar{\gamma}_{lj}\bar{\gamma}^{ik}\bar{D}_k\ln\psi\right)\\&=2K\psi^{-4}\left(2\bar{\gamma}^{il}\bar{D}_l\ln\psi-3\bar{\gamma}^{ik}\bar{D}_k\ln\psi\right)\\&=2K\psi^{-4}\bar{\gamma}^{il}\bar{D}_l\ln\psi \qquad (2.17b)\\\psi^{-4}K\bar{\gamma}^{il}C^{j}{}_{jl}&=2K\psi^{-4}\bar{\gamma}^{il}\left(2\delta^{j}{}_{(j}\bar{D}_{l)}\ln\psi-\bar{\gamma}_{lj}\bar{\gamma}^{jk}\bar{D}_k\ln\psi\right)\\&=2K\psi^{-4}\left(4\bar{\gamma}^{il}\bar{D}_l\ln\psi-\bar{\gamma}^{ik}\bar{D}_k\ln\psi\right)\\&=6K\psi^{-4}\bar{\gamma}^{il}\bar{D}_l\ln\psi\,. \qquad (2.17c)\end{aligned}$$

Finally, with (2.16a-2.16c) in the first term of (2.14) and (2.17a-2.17c) in the second one, the conformal momentum constraint equation is found to be:

$$\bar{D}_j\bar{A}^{ij}-\frac{2}{3}\psi^6\bar{\gamma}^{ij}\bar{D}_jK=8\pi\psi^{10}S^i\,. \tag{2.18}$$

This equation expresses the complementary information for the choice of K. Since (2.18) and (2.13) are coupled, we have to solve them simultaneously in order to determine all the referent objects lying in $\mathcal{T}$.

The formulation CTT is based on rewriting $\bar{A}^{ij}$ into its transverse and longitudinal parts. The transverse part is divergence-less and the longitudinal part is considered as gradient of some vector potential W^i. Thus, (2.18) takes the following form

$$\left(\bar{\Delta}_LW\right)^i-\frac{2}{3}\psi^6\bar{\gamma}^{ij}\bar{D}_jK=8\pi\psi^{10}S^i\,, \tag{2.19}$$

where the operator $\bar{\Delta}_L$ is given by:

$$\left(\bar{\Delta}_LW\right)^i\equiv\bar{D}_j\left(\bar{L}W\right)^{ij}\equiv\bar{D}_j\left(\bar{D}^iW^j+\bar{D}^jW^i-\frac{2}{3}\bar{\gamma}^{ij}\bar{D}_kW^k\right)\,. \tag{2.20}$$

Note that this definition of $\bar{L}$ keeps the trace-less property of $\bar{A}_{ij}$. A typical solution for W^i was given by Bowen and York in 1980. For the case of a boosted black hole in vacuum with an spacetime of $K = 0$, it follows from (2.19) that

$$\left(\bar{\Delta}_L W\right)^i = 0\,. \tag{2.21}$$

And its solution is [BS10, P.73]:

$$W^i = -\frac{1}{4r}\left(7P^i + l^i l_j P^j\right)\,, \tag{2.22}$$

where P^i is the black hole's linear momentum and l^j a normal vector pointing out from the singularity, i.e., $l^j = x^j/r$ with x^j and r the cartesian coordinates and radial isotropic coordinate, respectively. The solution (2.22) is used in chapter 3.1 in order to obtain $\bar{A}_{ij}$.

Once we have written the CTT system, it would be worth counting degrees of freedom (DOF). Just from the Ricci tensor in Einstein's equations we have twelve DOF. Then in ADM formulation those degrees are separated in two groups, six in γ_{ij} and six in K_{ij}. On the other hand, in CTT formulation there are other variables where DOF reside. Given (2.2a), the conformal factor has at most one degree and therefore $\bar{\gamma}_{ij}$ has five DOF. For the extrinsic curvature, from (2.8) and the conformal relations (2.9a) and (2.9b), we have that

$$K_{ij} = \psi^{-2}\left[\bar{A}^{(TT)}_{ij} + \bar{A}^{(LT)}_{ij}\right] + \frac{1}{3}\psi^{-4}K\bar{\gamma}_{ij}\,. \tag{2.23}$$

In (2.23), the six missing DOF must be allocated in K, $\bar{A}^{(TT)}_{ij}$ and $\bar{A}^{(LT)}_{ij}$. Since K is just a scalar, it can only account for one DOF. Also, we think of $\bar{A}^{(LT)}_{ij}$ as coming from a vector W^i, hence it should have at most three DOF and therefore, $\bar{A}^{(TT)}_{ij}$ contains the remaining two.

In order to determine those twelve DOF we have four equations, the hamiltonian and momentum constraint. In addition, we have freedom to choose a reference frame. There, we have three spatial and one temporal DOF. Thus, at the end we are stuck with four remaining DOF, two in $\bar{A}^{(TT)}_{ij}$ and two in $\bar{\gamma}_{ij}$. However, those degrees do

not enter in the CTT equations and hence are freely specifiable for this formalism. Nontheless, this freedom entails to different spacetime's evolutions and should be made conscientiously.

2.2 What about the gauge conditions?

Choosing appropriate gauge conditions is still one of the most intricate parts of numerical relativity. It is definitely the main difficulty in simulations for large timescales.

There exist several gauge conditions, with many comparisons made, but no ultimate decision on which is the best. What we want from those conditions is that they allow us to handle singularities (both physical and coordinate) and leave us with a stable system of equations. For example, in evolving the surrounding black hole spacetime we should keep out the overflows that appear close to singularities; or in gravitational collapse where initially there is no singularity but the system must end up with one.

The choice of lapse regulates how fast the system goes from one time slice to the next. Generally it depends on the spacetime coordinates. On the other hand, choosing the shift vector translates into how spatial points change respect to a normal time observer.

Geodesic slicing

One natural way to proceed is to follow a normal observer and let ourselves "go with the flow". In such case, we would expect the shift in space coordinates to be zero and there be unit lapse. This is known as geodesic slicing. These choices single out gravitational effects over other interactions. They follow star collapses correctly and even the Friedmann equations. However, geodesical simulations end or crash quickly [GMG06, BS10].

Figure 2.1 is a diagram representing the evolution of a Schwarzschild spacetime in Kruzkal Szekeres coordinates, taken from [SY78]. The top panel shows the case for geodesic slicing while the bottom panel is for maximal slicing. In both cases, the region to the right from the dashed line is the outside of the BH. This spacetime, where $r_{sch} \geq 2M$, is called region I. The sawtooth line represents the physical singularity, $r_{sch} = 0$. Region II, where $0 < r_{sch} \leq 2M$, lies inside the event horizon. In addition, this region represents the evolved spacetime. For geodesic slicing, the shaded region does not cover the entire external BH spacetime at the time that a geodesic touches the singularity. It does it with proper time corresponding to free falling time $\tau_{sch} = \pi M$. Thus, the simulation ends because of numerical overflow near the singularity before it completes the entire exterior. This means that short-time simulations, where the main interaction is gravitational, would be well resolved in this gauge.

Maximal slicing

This gague condition applies directly in the trace of the extrinsic curvature and leads to a behavior for lapse. The idea is to simplify equation (1.61b) using $K = 0$ for all time slices, hence $\partial_t K = 0$. In order to take advantage of the gauge, first we rewrite (1.61b) using $K_{ij} = \gamma_{jq} K^q_i$, therefore $\partial_t K_{ij} = \partial_t \gamma_{jq} K^q_i + \gamma_{jq} \partial_t K^q_i$. Then, with (1.61a) it follows that:

$$\begin{aligned} \gamma_{iq}\partial_t K^q_j &= -K^q_j \left(-2\alpha K_{iq} + 2D_{(i}\beta_{q)}\right) - D_i D_j \alpha + \alpha \left(R_{ij} - 2K_{il}K^l_j + KK_{ij}\right) \\ &\quad -8\pi\alpha \left[S_{ij} - \frac{1}{2}\gamma_{ij}\left(S - \rho\right)\right] + \beta^k D_k K_{ij} + 2K_{k(j}D_{i)}\beta^k \,. \end{aligned}$$

Now, factorizing γ_{iq} from the RHS and changing $q \to j$ we get:

$$\begin{aligned} \partial_t K &= 2\alpha K^{iq}K_{iq} - 2K^{iq}D_{(i}\beta_{q)} - D^j D_j \alpha + \alpha \left(R - 2K_{jl}K^{jl} + K^2\right) \\ &\quad -8\pi\alpha \left[S - \gamma^{ij}\gamma_{ij}\frac{1}{2}\left(S - \rho\right)\right] + \beta^k D_k K + K_{kj}D^j\beta^k + K^j_k D_j \beta^k \,, \end{aligned}$$

where the first term cancels out with the fifth, and the second the last two. In addition, since the trace of γ_{ij} is three, we have that for this gauge:

$$D^2\alpha = \alpha\left[R - 4\pi(3\rho - S)\right] \,. \tag{2.24}$$

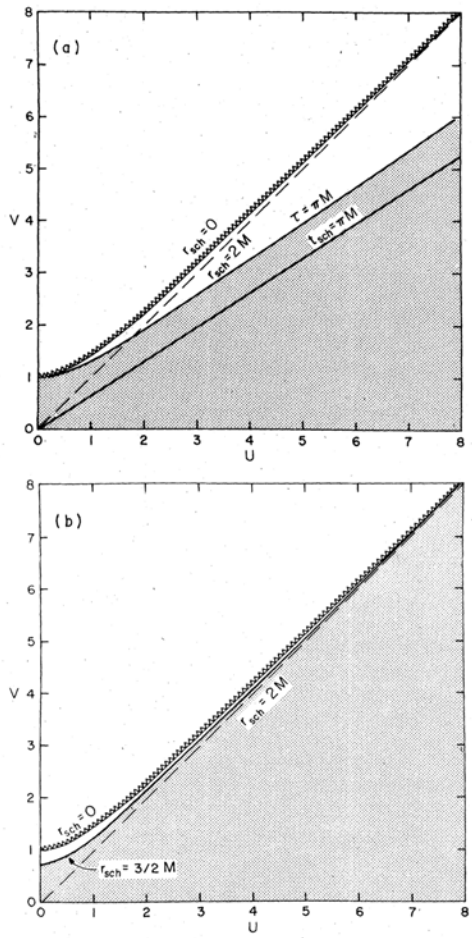

Figure 2.1: Geodesical Vs maximal slicing. Schwarzschild solution in Kruskal Szekeres coordinates (u, v), part of regions I and II. Top panel with geodesic slicing and bottom panel with maximal slicing. In both panels the dashed line is the coordinate singularity $r_{sch} = 2M$ while the sawtooth line is the physical singularity $r_{sch} = 0$. The shaded regions represent an evolved spacetime for a numerical evolution of initial time slice $v = t_{sch} = 0$. Taken, with permission, from [SY78].

This equation doesn't give a condition for β^k and could be solved independently. Foliations under condition (2.24) have the next geometrical meaning: given that K is related to the divergence of normal observers, as seen in (1.28), $K = 0$ implies a non changing separation between observers, and leads to the preservation of proper 3D-volume. Because n^a is irrotational, the above guarantees that normal observers move in irrotational and incompressible fluid elements, i.e., in a perfect fluid. This incompressible property

is given by the acceleration of the normal observers, $D^2\alpha$, which prevents the focusing that leads to a crash in the numerical evolution.

In the bottom part of figure 2.1, we see the simulation for a evolved Schwarzschild spacetime with a maximal gauge condition. Recalling the relationship between Schwarzschild time and Kruskal Szekeres coordinates [BS10, P.12]

$$t_{sch} = 4M \operatorname{Arctanh} \frac{v}{u} \qquad \text{(for region II)}\,,$$

we notice that the evolved spacetime covers the entire external region of the BH as time $t_{sch} \to \infty$. In addition, for these coordinates there is no singularity in $r_{sch} = 2M$, so we can actually see the evolved spacetime going inner to event horizon. An imporatnt gauge's property is also shown in the figure, the shaded regions asymptotically approaches the physical singularity. It becomes stationary at $r_{sch} = \frac{3M}{2}$, then the evolution becomes time independent [BS10, Sec.4.2]. This singularity avoidance makes maximal slicing a good condition for long term simulations.

For the Schwarzschild solution τ is related to t_{sch} by α, and we also know that $t_{sch} \to \infty$ as we approach to $r = 0$. However, the proper time remains finite. Therefore, alpha must go to zero in order to maintain a finite value of τ. This is one frequently noted feature in numerical simulations [HECB03, BS10] and is called "collapse of lapse". This behavior is usually used in solving (2.24) as condition for evolving γ_{ij} and K_{ij} [GGB02].

With the aim to get analytical results, in [BY80] they used a conformal mapping of the form $\psi = \frac{a}{r}\bar{\psi}$ to show that when the conformal metric is flat the volume is an extremal for $r = a$. Therefore, the trace of the extrinsic curvature for a 2D-surface $f(a, \theta, \phi)$, regarded as a surface embedded in the conformally flat 3D-space, vanishes. Indeed, they show that maximal gauge is responsible for a minimal spatial volume, hence leading to a maximal 4D-volume and to its name.

Harmonic slicing

Harmonic slicing is the gauge condition that allowed to carry over Einstein's equations in the 3+1 formalism to simulations in fluid dynamics [BMSS95]. In spite of the fact that the field variables become unstable near of singularities for this gauge. This gauge is used because it's easy to implement. Also, in avoiding singularities, harmonic slicing is placed between geodesic and maximal slicing [SN95, GMG06]. Recently, a variation of harmonic slicing gave numerical simulations as stable as those using maximal slicing [IB09]. This is the main reason why it was a popular choice for work on the merger of binary neutron system [IB09, BHS99].

The harmonic slicing gauge is obtained by assuming conditions over the contraction of the 4D-connection symbols, $\Gamma^a = g^{bc}\Gamma^a_{bc}$, and shift vector

$$\Gamma^0 = -\frac{1}{\sqrt{g}}\partial_b\left(\sqrt{g}g^{0b}\right) = 0 \tag{2.25a}$$

$$\beta^i = 0\,, \tag{2.25b}$$

using (2.25b) in the metric (1.59d) we get that $\sqrt{g} = \alpha\sqrt{\gamma}$, so (2.25a) gives

$$\Gamma^0 = \frac{1}{\alpha\sqrt{\gamma}}\partial_t\left[\alpha^{-1}\sqrt{\gamma}\right] = -\alpha^{-2}\partial_t\alpha + \frac{\alpha^{-1}}{\sqrt{\gamma}}\partial_t\sqrt{\gamma} = 0\,.$$

By taking the trace of (1.61a) and using that $\frac{1}{2}\gamma^{ij}\partial_t\gamma_{ij} = \gamma^{-\frac{1}{2}}\partial_t\gamma^{\frac{1}{2}}$, [Cha13, P.86], we have the slicing condition over the lapse

$$\partial_t\alpha = -\alpha^2 K\,. \tag{2.26}$$

The origin of this gauge's name is due to the fact that it's a variation of the harmonic coordinate gauge condition, in which all the components of Γ^a are zero. Hence, the coordinates follow the 4D-Laplace equation with harmonic solution [BS10, P.112].

A different approach followed by [BMSS95] leads to a more general harmonic slicing; this work is focused in getting the most general condition for α such that the evolution equations end up in a strongly hyperbolic form. The condition's expression for lapse,

using $\beta^i = 0$, should obey

$$\partial_t \alpha \; = \; -\alpha^2 f(\alpha) K \, , \tag{2.27}$$

where $f(\alpha)$ should belong to $(1, 2)$. Moreover, different values of $f(\alpha)$ give earlier gauge conditions, e.g., $f = 1$ and $f = 0$ lead to harmonic and geodesic slicing, respectively. For maximal slicing, given the collapse of the lapse, we expect that $f \to \infty$.

Minimal distortion

Although, the slicing gauge has proven to be a good choice for some numerical evolution, we have not said anything about the condition for the shift vector β^i yet. Indeed, there are not many choices because $\beta^i = 0$ leads to good simulations. As more simulations were explored and systems were diversified, more evident was the need for another shift condition; specially in geometries around rotating massive bodies [BS10, Alc08, GMG06].

A popular framework is to minimize those changes due to unphysical degrees of freedom in $\bar{\gamma}_{ij}$. Moreover, this condition applies over $\partial_t \bar{\gamma}_{ij}$ rather than $\bar{\gamma}_{ij}$. Using a separation of longitudinal and transverse parts of $\partial_t \bar{\gamma}_{ij}$, like that in section 2.1, the longitudinal one corresponds to a symmetric trace-less gradient for some one-form X_k

$$u_{ij}^{(TL)} \equiv \partial_t \bar{\gamma}_{ij}^{(TL)} = D_i X_j + D_j X_i - \frac{2}{3} \gamma_{ij} D^k X_k \, . \tag{2.28}$$

Finally, using (2.2b) in (2.28), leads to

$$\begin{aligned} u_{ij}^{(TL)} &= \gamma^{1/3} \left(\bar{\gamma}_{kj} D_i X^k + \bar{\gamma}_{ik} D_j X^k - \frac{2}{3} \bar{\gamma}_{ij} D_k X^k \right) \\ &= \gamma^{1/3} \mathcal{L}_{\vec{X}} \bar{\gamma}_{ij} \, , \end{aligned} \tag{2.29}$$

i.e., $u_{ij}^{(TL)}$ is related to changes of $\bar{\gamma}_{ij}$ along $\vec{X}$. In such form, from (1.23) we identify that case $u_{ij}^{(TL)} = 0$ implies no change for $\bar{\gamma}_{ij}$ along $\vec{X}$, i.e., $\vec{X}$ is a *conformal Killing vector* and (2.29) leads to the conformal Killing equation for $\bar{\gamma}_{ij}$. Besides, it means that $\bar{\gamma}_{ij}$ has $Dim(\mathbf{X}) -$ symmetries. If $\vec{X}$ is related to our coordinates set, the evolution

of $\bar{\gamma}_{ij}$ should be free of changes coming from coordinates, which in principle are free choices.

There are several more gauges to explore and we stress that choosing one depends on which is favorable for the simulation. None of them have physical information but picking up the one which fit will makes the work easier. However, since in this work we don't evolve γ_{ij} or K_{ij}, we leave this discussion here and continue on our main goal of setting up their initial conditions.

2.3 Methodology

We already have discussed the basic ideas of how Einstein's equations emigrate to a new form in 3+1 NR. Now, in order to work in the subject we need information about the physical system we want to simulate. Therefore, from this section on we work with the following system: a boosted black hole (BBH) in equilibrium, represented as a trumpet geometry rather than a wormhole (discussed below).

Using equilibrium solutions implies that the changes related to global time are zero, and from (1.28) we know that the spacetime follows a maximal slicing condition

$$K = 0\,. \tag{2.30}$$

Moreover, this system is used in [IB09], where in addition they propose to employ conformal flatness, i.e.

$$\bar{\gamma}_{ij} = \eta_{ij}\,. \tag{2.31}$$

This is a popular decision and we take it since that leads to Bowen York solutions. The equations are handled in CTT formalism and solved using the punctures approach, as discussed below. This setup is a toy model example for working in 3+1 NR and for that reason it's useful to us. We will justify the CTT and the punctures choices that we just made based on a few earlier published papers.

2.3.1 Why punctures ?

Singularities are one of the most important issues to attend in the process of solving numerical equations. Because of their physical and numerical importance in relativity, and that they are so common, we better use a method which handle them properly.

The first idea to handle singularities was the use of different coordinate systems such that the equations became easier to integrate; under that scheme, conditions were made on the lapse function and shift vector. As a result, the singularities were postponed to enter in the calculation until late times in the evolution. For example, maximal slicing conditions generate a singularity when the time coordinate goes to infinity, so it is a proper gauge to explore gravitational collapse. For short time simulations like head-on collisions, coordinate avoidance like geodesic slicing has proven to be sufficient, however for long-time mergers they are not. This is why other methods have been introduced, namely excision and punctures [**?**, Alcubierre,Shapiro] The former has been used since the 80's and it's based on the cosmic censorship. This assures that every physical singularity should be covered by an event horizon. Hence, any information coming from nearby the singularity could be irrelevant for the outside region. Therefore, it's enough to use only the outside region for the evolution excising the inner region. This sounds easy to work out, yet in practice some troubles pop up. For example, identifying where the event horizons reside is an important one, for this we need to know the whole information about the spacetime, which in principle is unknown [BS10]. Afterward, we have to decide if we interpolate the closest data to the event horizon or use an appropriate method for the region of interest.

On the other hand, the punctures method was originally stated as an alternative to excision by D. Brill and R. Lindquist (1963). Having in mind those problems on the BH inner boundary for lapse and shift conditions (see next section), the motivation for the punctures method is not to use the region involving the BH horizon. Instead, use

two a part solution. One part being an analytic but irregular already known solution, this is the background geometry of the singularity. The other part is a correction term, usually named u, which has to be numerically solved.

Following the above idea, u should be regular in the whole spacetime, however, it is most useful near the puncture. Then, the entire solution is a superposition of a puncture around the singularity, given by the analytic part ψ_0, and u containing the behavior far from the singularity. As we see in chapter 3, this leads to rewriting the ψ equation in terms of u. Thus, the problem of finding initial conditions is translated to find the regular function u.

Now, let's turn to explain why we use trumpet geometry instead of Schwarzschild solution and what's the difference between these two.

2.3.2 Trumpet geometry and CTT approach

As we discuss in (2.2), making use of maximal slicing gauge entails solving (2.24) for α in order to evolve the system. However, without clear boundary conditions it can be solved up to a parametric family of functions for α. In particular, for a spherical symmetric case when α is assumed to be time independent, it turns out that [BS10, P.106]:

$$\alpha(r_{sch}; C) = \pm\sqrt{1 - \frac{2M}{r_{sch}} + \frac{C^2}{r_{sch}^4}}\,. \tag{2.32}$$

Since this equation is valid for spherical and time independent spacetimes, we can compare it with the α for the Schwarzschild solution in order to identify C. Thus, the line element for the Schwarzschild solution in Schwarzschild coordinates is [HEL06, P.201]:

$$ds^2 = -\left(1 - \frac{2M}{r_{sch}}\right) dt^2 + \left(1 - \frac{2M}{r_{sch}}\right)^{-1} dr_{sch}^2 + r_{sch}^2 d\theta^2 + r_{sch}^2 \sin^2\theta d\phi^2\,.$$

From (1.59d) we get:

$$\alpha(r_{sch}) = \pm\sqrt{1 - \frac{2M}{r_{sch}}}\,, \tag{2.33}$$

where $C = 0$ leads to the lapse function for the Schwarzschild solution. From this, we have a better picture of the infinite possibilities we have in choosing a coordinate system; i.e., all of the choices accomplishing (2.32) lead to a maximal slicing spacetime, besides, every choice implies a different geometry with different coordinates.

There is one particular value for C such that the system ends stationary, $C = \frac{3\sqrt{3}M^2}{4}$. Unlike Schwarzschild coordinates, this value for C makes the lapse collapse at the minimal radius $r'_{sch} = \frac{3M}{2}$. Only those two C's values lead to a time independent solution [BS10], but they represent different geometries. The first one is two-flat ends spacetime connected by a throat. The second one is just a flat end connected to the throat of minimal radius.

Now, in order to see why we choose the CTT approach, we need to present another one that we didn't mention until now, the Conformal Thin Sandwich decomposition (CTS). We just worked out the CTT formalism since that's the one we use here, however it's important to notice why we stay in CTT and not CTS for this work.

The main difference in the CTS is that it works with time derivatives of $\bar{\gamma}_{ij}$ and K, rather than their values in $\mathcal{T}_0$, hence its name. Then, in CTS the definition for the trace-less time derivative of γ_{ij} is the feature equation:

$$u_{ij} = \gamma^{1/3}\partial_t\left(\gamma^{-1/3}\gamma_{ij}\right) . \tag{2.34}$$

For a given u_{ij} we can use (1.61a) and solve (2.34) for $\bar{A}^{ij}$, that is:

$$\bar{A}^{ij} = \frac{1}{2\bar{\alpha}}\left(\left(\bar{L}\beta\right)^{ij} - \bar{u}^{ij}\right), \tag{2.35}$$

where

$$\alpha = \psi^6\bar{\alpha}\,, \quad (L\beta)^{ij} = \psi^{-4}\left(\bar{L}\beta\right)^{ij} \quad \text{and} \quad u^{ij} = \psi^{-4}\bar{u}^{ij}\,. \tag{2.36}$$

Then, with (2.35) into hamiltonian and momentum constraints we end up with a new system of equations including α and $\vec{\beta}$, namely the CTS equations. So, in CTS the initial values for α and $\vec{\beta}$ are found solving the equations rather than choosing them.

For that reason, we expect that using CTS would be better in obtaining initial values than CTT. But it turns out to be complicated when we use the punctures method.

As we saw in section 2.2, α has a collapsing behavior near of the event horizon. Therefore, from (2.35) this takes $\bar{A}^{ij}$ to unstable values. In [HECB03] they worked on what was the issue for this problem and their result is not a good answer for CTS + Punctures. They find that α should vary for different regions and once it has passed the BH throat its sign must change, refer to (2.32). This change of sign implies a zero value for α, hence for $\bar{\alpha}$, which is terrible for the CTS equations. This problem is solved in [BM94], its solution involves imposing values on $\vec{\beta}$ for the inner boundary which makes $\bar{A}^{ij}$ regular. However, this is the intention of the punctures method: it is proposed to avoid finding the event horizons.

Chapter 3 | *A CTT's application*

In this chapter we discuss the issues of solving the constraint equations (2.13) and (2.18) for a boosted black hole. In particular we want to obtain a conformal factor developed in [IB09]. In this article they use the punctures method to recover some results which already have been calculated under the excision method. Nonetheless, using the punctures method is easier since there is no need to specify the inner boundary conditions.

3.1 Solving the hamiltonian constraint

Given that we have a constant K and that a black hole exterior is regarded as empty, the momentum constraint (2.18) decouples from the hamiltonian (2.13). This is

$$\bar{D}_i \bar{A}^{ij} = 0\,. \tag{3.1}$$

Therefore, we can solve it for $\bar{A}^{ij}$. Indeed, this is (2.21), and the general solution was given by Bowen and York in [BY80]. From (2.22) it follows that:

$$\bar{A}^{ij} = \frac{3}{2r^2}\left[P^i l^j + P^j l^i - \left(\bar{\gamma}^{ij} - l^i l^j\right) l_k P^k\right]\,, \tag{3.2}$$

where P^i is the black hole's linear momentum and l^j is a normal vector pointing out from the singularity, i.e., $l^j = x^j/r$ with x^j and r the cartesian coordinates and radial isotropic coordinate, respectively. As we noticed in (2.3.1) the conformal factor and $\bar{A}^{ij}$ are written as

$$\psi = \psi_0 + u \tag{3.3a}$$

$$\bar{A}^{ij} = \bar{A_0}^{ij} + \bar{A_p}^{ij}\,, \tag{3.3b}$$

with u being the regular part of ψ. ψ_0 is the irregular part and contains the information about the trumpet geometry. On the other hand, $\bar{A}_0{}^{ij}$ and $\bar{A}_p{}^{ij}$ are associated to the background extrinsic curvature (Schwarzchild trumpet) and to one generated by the boosted black hole.

The background conformal factor is given by the trumpet geometry, it has the lapse function like (2.32) and is time independent, [IB09, HHM09, BS10]. However, to use the conformal approach we have to rewrite the 3D-metric as having a global factor, (2.2a). In [BN07] they found that ψ_0, as written in isotropic coordinates, is related to the areal radius r_{sch} by

$$\psi_0{}^4 = \left(\frac{r_{sch}}{r}\right)^2 , \tag{3.4a}$$

where r and r_{sch} are related as

$$\begin{aligned} r &= \left[\frac{2r_{sch} + M + \sqrt{4r_{sch}^2 + 4Mr_{sch} + 3M^2}}{4}\right] \times \\ &\qquad \left[\frac{(4+3\sqrt{2})(2r_{sch} - 3M)}{8r_{sch} + 6M + 3\sqrt{8r_{sch}^2 + 8Mr_{sch} + 6M^2}}\right]^{\frac{\sqrt{2}}{2}} . \end{aligned} \tag{3.4b}$$

Given the structure of this equation, they argue that an inverse for $r_{sch} = r_{sch}(r)$ is not analytically possible. However, several researches have verified that (3.4b) has the desired corresponding limits [BN07, IB09]:

$$\psi_0 \to \begin{cases} \sqrt{\dfrac{3M}{2r}} \quad \text{as} \quad r \to 0 \quad \text{(Trumpet)} & \text{(3.5a)} \\ 1 + \dfrac{M}{2r} \quad \text{as} \quad r \to \infty \quad \text{(Swcharzschild)} . & \text{(3.5b)} \end{cases}$$

From these limits and (3.4a), we see that the singularity $r = 0$ in (3.5a) corresponds to $r_{sch} = r'_{sch}$ in Schwarzschild coordinates, so it's a mere coordinate singularity. Moreover, in order to describe an asymptotic flat spacetime, we recall from (2.2a) that we should have $\psi_0 \to 1$ as $r \to \infty$. In that limit r_{sch} must behave like r and hence it follows that $r_{sch} \to \infty$ as $r \to \infty$.

We take the background's extrinsic trace-less curvature like the one proposed in [HHM09, IB09] for the trumpet geometry

$$\bar{A}_0^{ij} = \frac{C}{r^3}\left(\bar{\gamma}^{ij} - 3l^i l^j\right) \; ; \qquad C = \frac{\sqrt{27}M^2}{4} \, . \tag{3.6}$$

From here we can notice that $\bar{A}_0^{ij}$ has null trace. Moreover, writing it explicitly we check that it obeys (3.1):

$$\begin{aligned} \frac{1}{C}\bar{D}_i\bar{A}_0^{ij} = \frac{1}{C}\partial_i\bar{A}_0^{ij} &= \partial_i\left(-\eta_{kl}x^k x^l\right)^{-\frac{3}{2}}\left[\eta^{ij} - 3x^i x^j\left(-\eta_{kl}x^k x^l\right)^{-1}\right] \\ &\quad + \partial_i\left[\eta^{ij} - 3x^i x^j\left(-\eta_{kl}x^k x^l\right)^{-1}\right]\left(-\eta_{kl}x^k x^l\right)^{-\frac{3}{2}} \, , \end{aligned}$$

where

$$\partial_i\left(-\eta_{kl}x^k x^l\right)^{-\frac{3}{2}} = -\frac{3}{2}\left(-\eta_{kl}x^k x^l\right)^{-\frac{5}{2}}(2x_i) = -\frac{3x_i}{r^5}$$

and

$$\begin{aligned} \partial_i\left[\eta^{ij} - 3x^i x^j\left(-\eta_{kl}x^k x^l\right)^{-1}\right] &= -3\partial_i\left[x^i x^j\left(-\eta_{kl}x^k x^l\right)^{-1}\right] = 3\left[\frac{4}{r^2} + \frac{1}{r^4}x^i x^j\left(x_k\delta_i^k + x_l\delta_i^l\right)\right] \\ &= 3\left(\frac{4}{r^2} - \frac{2}{r^2}\right)x^j = \frac{6x^j}{r^2} \, . \end{aligned}$$

By pulling all together we arrive at (3.1):

$$\frac{1}{C}\bar{D}_i\bar{A}_0^{ij} = -\frac{3x_i}{r^5}\left(\eta^{ij} - 3\frac{x^i x^j}{r^2}\right) - \frac{6x^j}{r^5} = -\frac{3x^j}{r^5} + \frac{9x^j}{r^5} - \frac{6x^j}{r^5} = 0 \, .$$

From this result we see that adding as many terms of $\bar{A}_{ij}$ as we need doesn't change the constraint equations. For this reason we conclude that this procedure leads to an acceptable solution.

Now, expressing (2.13) in terms of (3.3), and using the background solution,

$$\bar{D}^2\psi_0 + \frac{1}{8}{\psi_0}^{-7}\bar{A}_0^2 = 0 \, , \tag{3.7}$$

we have

$$\bar{D}^2 u - \frac{1}{8}{\psi_0}^{-7}\bar{A}_0^2 + \frac{1}{8}\left(\psi_0 + u\right)^{-7}\left(\bar{A}_0^2 + 2\bar{A}_{0p}^2 + \bar{A}_p^2\right) = 0 \, , \tag{3.8}$$

where

$$\bar{A}_0^2 \equiv \bar{A}_0^{ij}\bar{A}_{0ij} \, , \quad \bar{A}_p^2 \equiv \bar{A}_p^{ij}\bar{A}_{pij} \quad \text{and} \quad \bar{A}_{0p}^2 \equiv \bar{A}_0^{ij}\bar{A}_{pij} \, . \tag{3.9}$$

In order to calculate these objects we should use $\bar{\gamma}_{ij}$ to take down the indices of (3.2) and contract them on themselves. That is a big task and one often makes mistakes along the calculation. Fortunately, there are a few packages for symbolic calculation software to do so. Here we use *xAct* package ([Me]) on *Mathematica*© V. 9 to workout the terms (3.9).

At Appendix B.1 we shed light on the procedure to obtain the values for $\bar{A}_0$, $\bar{A}_p^2$ and $\bar{A}_{0p}^2$. Their values are:

$$\bar{A}_0^2 = \frac{81}{8}\frac{M^4}{r^6} \tag{3.10a}$$

$$\bar{A}_{0p}^2 = -\frac{27\sqrt{3}}{4}\frac{M^2 P\cos\theta}{r^5} \tag{3.10b}$$

$$\bar{A}_p^2 = \frac{9}{2}\frac{P^2}{r^4}\left(1+2\cos^2\theta\right), \tag{3.10c}$$

where

$$P = \left(\bar{\gamma}_{ij}P^iP^j\right)^{\frac{1}{2}} \quad \text{and} \quad \cos\theta = \frac{\bar{\gamma}_{ij}P^i l^j}{|\bar{\gamma}_{ij}P^i l^j|}\,. \tag{3.11}$$

Notice that (3.8) in terms of (3.10a)-(3.10c) seems to be the kind of electrostatic problem where an electrical dipole interacts with an electric field. In there, we usually orient the electric field along z axis and recover an expression independent of the dipole's direction. However, the non-linearity of $\{u,\psi_0\}$ in (3.8), and the complexity to find $r_{sch}(r)$ from (3.4b) left us with no choice but a numerical approximation for u. In that case, it might be useful to analyze (3.8) first.

Since our relevant region for u is the punctures' nearby, let's take the regions where $r\to 0$.

Given that u is regular, we are able to expect that $\psi_0 >> u$ for this regime. Thus, from (3.8) and at first order in u, we have the conformal factor's behavior around the puncture:

$$\begin{aligned}\bar{D}^2u &\approx -\frac{1}{8}{\psi_0}^{-7}\left(1-\frac{7u}{\psi_0}\right)\left(\frac{81}{8}\frac{M^4}{r^6}-\frac{27\sqrt{3}}{4}\frac{M^2P\cos\theta}{r^5}\right)+\frac{1}{8}{\psi_0}^{-7}\frac{81}{8}\frac{M^4}{r^6}\\ &\approx \frac{1}{\sqrt{2}}\left(\frac{M}{r}\right)^{\frac{3}{2}}\frac{P\cos\theta}{M^3}+\frac{7}{4}\frac{u}{r^2}\,.\end{aligned} \tag{3.12}$$

Here we have used the limit (3.5) and neglected the contributions from $\bar{A}_p^2$ since the others' denominator have more impact. Actually, we see from (3.12) that the u's requirement to be regular is

$$u_{\text{punc}} = 0 \quad ; \quad r = 0\,. \tag{3.13}$$

To find the solution of (3.12) we used the Finite Sturm-Liuville Transform (FSLT) introduced in [ERI54]. The procedure is at Appendix C, and the u solution is:

$$u\left(\vec{r}\right) = -\frac{1}{3\sqrt{2}}\frac{P\cos\theta}{M^{\frac{3}{2}}}r^{\frac{1}{2}} + \sum_{m=0}^{\infty} C_m r^{-\frac{1}{2}\left(1-2\sqrt{2+m(m+1)}\right)} P_m\left(\cos\theta\right)\,, \tag{3.14}$$

where only the boundary condition (3.13) was used. In order to determine the C_m coefficient we should give a behavior of u or its derivative respect to r around the puncture, usually a Robin condition is applied for that. We don't do the latter by now since the (3.12) is thought for origin close regions. Thus, we expect that u barely touch the middle zone in r. Instead, we point out that the most notorious contribution in the solution (3.14) is given by its first term, this is called the "limit solution"

$$u_L\left(\vec{r}\right) = -\frac{1}{3\sqrt{2}}\frac{P\cos\theta}{M^{\frac{3}{2}}}r^{\frac{1}{2}}\,. \tag{3.15}$$

Using this equation with the limit (3.5a) into (3.3a) would give us how the conformal factor behaves close to the puncture. Thus, a behavior for the 3D-metric and the extrinsic curvature near the black hole can be found, see figure 3.1. However, it is just a part of what we want. A next step to improve the solution is proposed in [IB09]. In there, they bring out the following iterative equation for u

$$\bar{D}^2 u^{N+1} = -\frac{1}{8}\left(\psi_0 + u^N\right)^{-7}\bar{A}^2 + \frac{1}{8}\psi_0^{-7}\bar{A}_0^2 + \frac{7}{8}\psi_0^{-8}\bar{A}_0^2\left(u^{N+1} - u^N\right)\,. \tag{3.16}$$

In this equation we should solve u^{N+1} for an u^N given. Thus, after inserting u^{N+1} back into the equation, now as u^N, we should solve again the differential equation for a new u^{N+1}. It has to be clear that the obtained solution is an array and its entries are the evaluation of u^{N+1} at discrete coordinate values $\{r, \theta\}$. Thus, in the convergence limit where $u^{N+1} \approx u^N$, the equation (3.16) reduces to (3.8) and its solution to the one we want.

3.2 Results

The equation (3.16) is a second order linear PDE and there are several methods to find a numerical solution. The region of interest is bounded by $r = 0$ and $r \to \infty$. In the former, we already have the boundary condition (3.13). And in order to obtain $\psi \to 1$ as $r \to \infty$, the natural condition for the latter would be $u \to 0$. However, to compare our solution to the one in [IB09], we use the following Robin boundary condition

$$\partial_r(ru) = 0 \qquad \text{for any} \quad 0 < r < \infty\,. \tag{3.17}$$

Our numerical approximation is found using a second order centered Finite Differences Method (FDM). The procedure to solve (3.16) is at Appendix B.2. The solution u^{N+1} differs from u^N at most in 1×10^{-6} for $N = 7$. In order to compare the solution with (3.15) in figure (3.1) we show u along z axis.

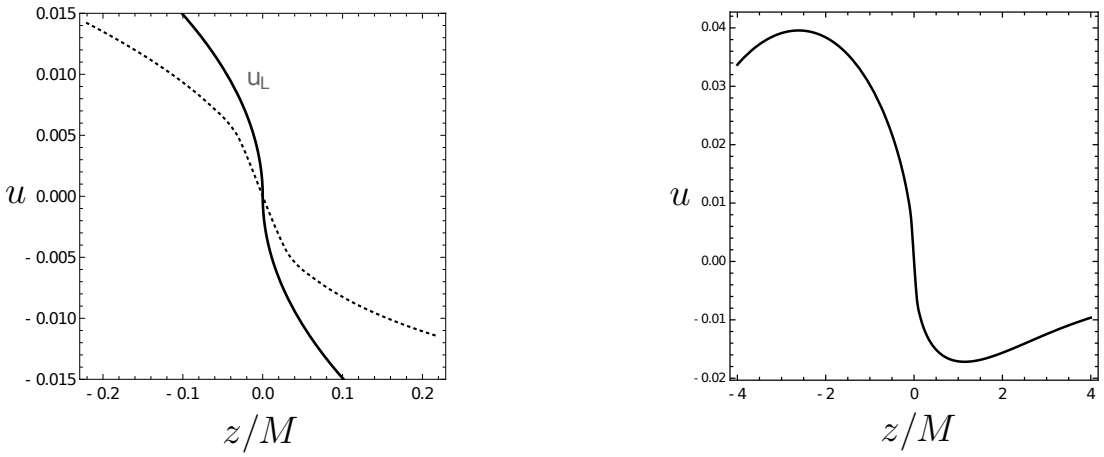

(a) **(b)**

Figure 3.1: u solution along z axis. The x and y axes have been suppressed in order to show the behavior in θ. Both cases have $\Delta z = M/16$ with a maximal error about of 10^{-6}. In 3.1a we compare the limit solution u_L (continuous line) with the numerical result (dashed line). For 3.1b we show the entire region numerical solution as a continuous line, $|z| \leq 4$.

From figures 3.1 and 3.2 we may notice a couple of things. First, the solution is symmetric in x-axis, and since the equation (3.8) has axial symmetry in z, the same is expected for y-axis. Second, the used condition, (3.17), doesn't allow to reach a zero

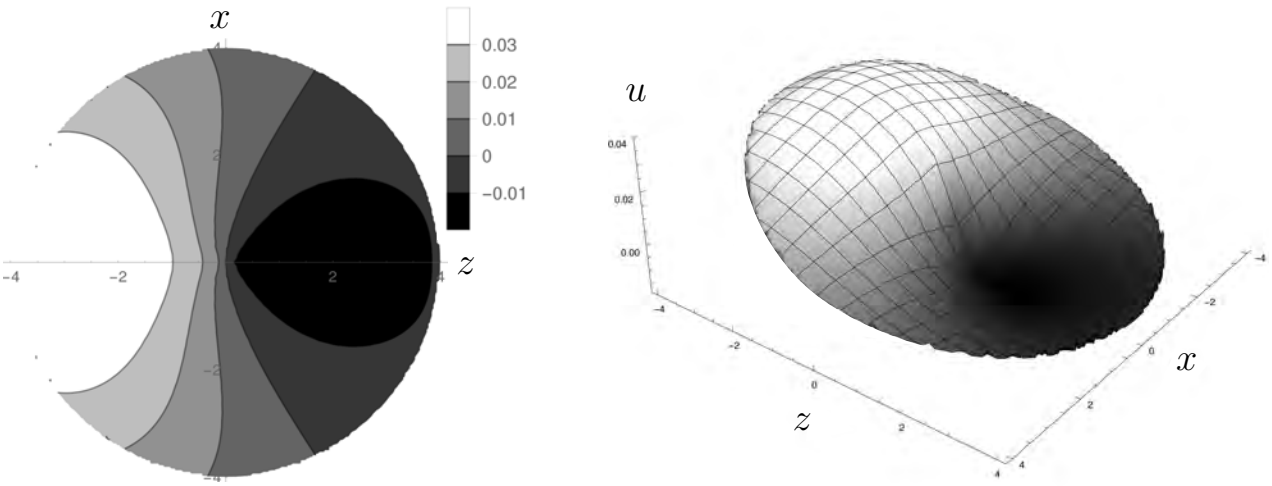

(a) **(b)**

Figure 3.2: Contour and 3D plot of u solution with y axis suppressed. Notice the symmetry along x axis.

value for u. As we see in the figure 3.1b, the u outer values tend to stabilize rather than go to zero, therefore this condition deserves attention in further works. The results shown in figure 3.1a are in agreement with [IB09].

The limit solution (3.15) into (3.3) gives us a limit conformal factor which has the form

$$\psi_L = \psi_0 \left(1 - \frac{r l^i P^j \delta_{ij}}{3\sqrt{3}M^2}\right) . \tag{3.18}$$

From this equation we see that $z/M = 3\sqrt{3}(M/P)$ leads to a collapse of the conformal factor. In there, the 3D-metric would be zero and the extrinsic curvature goes to infinity. Even though this is a serious thing, we notice that for $P = 0.2M$ (figure 3.1a) the z/M value is roughly 26. However, the region solution is $|r/M| \leq 4$ and then this implication is uncertain. On the other hand, for $P = 2M$ we get $z/M \approx 2.6$, which is within the region solution. Although, keeping in mind that this result is expected for radiuses close to zero, from the figure 3.3 we delimit the validity of u_L by comparing it with u. This gives us the actual effective radius' values $|z/M| \leq 0.3$. Moreover, from figure 3.3b we notice that no P values lead to the above results. This change in the

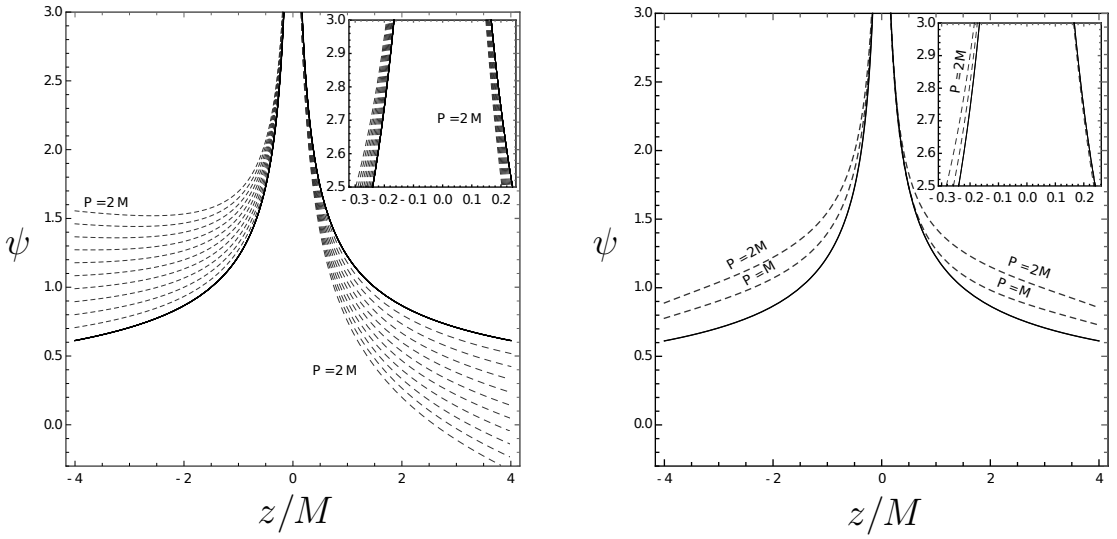

(a) **(b)**

Figure 3.3: Conformal factor for different linear momenta. The black continuous line is the case for the Schwarzschild solution, $P = 0$. 3.3a shows the limit conformal factor using u_L, while 3.3b uses the numerical solution u. The inset graphics help notice the region where those conformal factors agree. Dashed curves furthest to the left correspond to solutions for $P = 2M$ and as the go to the right they take lower P values approaching zero in 3.3a and M in 3.3b.

behavior should be a consequence of those not involved terms in u_L, (3.14). However, the asymmetry of the solution in z-axis still remains, this may implies that objects in direction of the linear momentum $\vec{P}$ are less affected by the BBH than those in back.

Another important feature that we observe in the numerical solution is that it behaves like (3.5a), which is the idea of punctures method (see figure 3.3b). On the other hand, the limit (3.5b) is not recovered because we used (3.5a) in (3.8) to solve it for u. In order to obtain a general solution which includes both limits (3.5), we have to invert (3.4b) for r_{sch} and use it into ψ_0. To do so, in [BN07] it's proposed to use an approximation rather than an analytical inversion:

$$r = r_{sch}\left(1 - \frac{M}{r_{sch}} - \frac{M^2}{2r_{sch}^2}\right) . \tag{3.19}$$

This equation can be solved for $r_{sch}(r)$ whit the following results:

$$r_{sch} = \frac{1}{2}\left(M + r \pm \sqrt{3M^2 + 2Mr + r^2}\right) , \tag{3.20}$$

the sign minus leads to negative r_{sch} values for any M, thus we should take the other one. Using this radius in (3.4a) we can solve (3.16) for a more general solution, namely u_s. The result for different momentum values are shown in figure 3.4. We notice that u_s behaves like both limits (3.5). For z values close to zero the behavior of u and u_s seems to be the same, see figure 3.4a. However, as we pointed out u_s doesn't go to zero for last radius' values and hence the conformal factor in figure 3.4b doesn't get the expected value for the limit (3.5b), which for the case is $\psi_0(4M) \approx 1.125$.

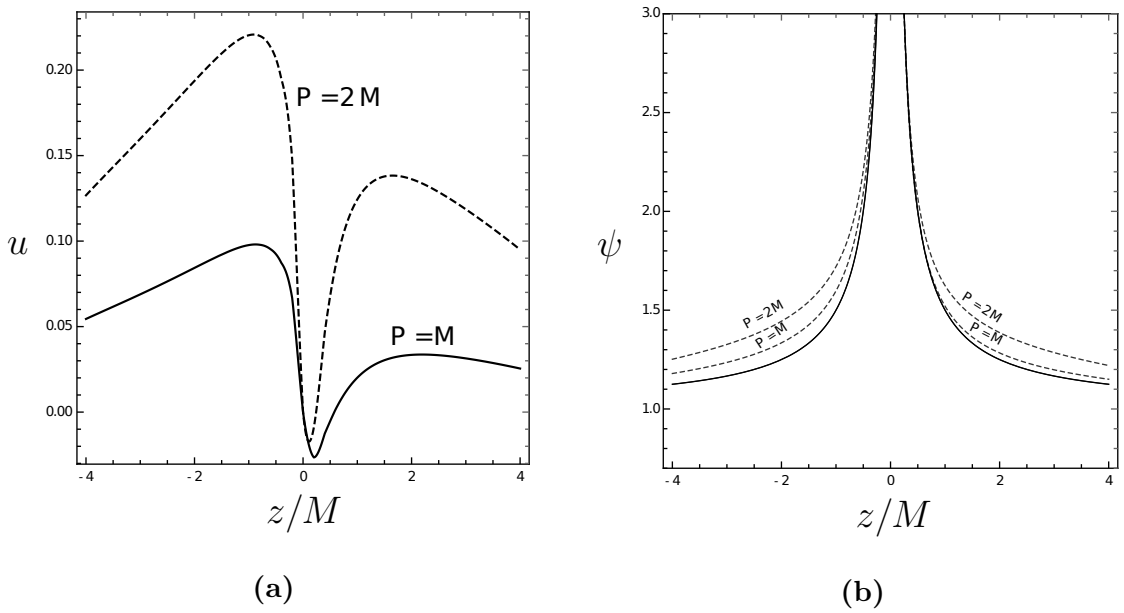

(a) **(b)**

Figure 3.4: Numerical solution using the r_{sch} approximation (3.20). 3.4a is the u_s's behavior while 3.4b corresponds to the conformal factor. In the latter, the dashed lines correspond to solutions with $P = \{M, 2M\}$.

Conclusions and further work

Along this work we have passed trhough the ADM and CTT approaches, both of them embedded into the 3+1 numerical relativity.

In the first part of the work we see that Einstein's equations can be separated in two sets. However, only one of them depends on time. These sets of equations take a particular form once we define the 3D-metric and the extrinsic curvature tensors, which are the field variables and we have to find them in the ADM approach. Therefore, they have physical meaning: the 3D-metric describes the geometry for any fixed value of the time. On the other hand, the extrinsic curvature describes the temporal changes on the 3D-metric. Thus, if the 3D-metric does not have time dependence, i.e., it's stationary, the extrinsic curvature tensor is null.

In the second part we noticed that by using a conformal mapping in the field variables, the constraint equations can be taken in such structure that it allows to exploit the conformal mapping. Not all of the spacetimes have this property but the one we employed here does. This is related to the Schwarzschild spacetime in isotropic coordinates. An important simplification can be made by taking the background metric as flat. Thus, the differential operators take an easier form and lead to simplify the constraint equations.

Once the conformal factor is found, it is used to transform the conformal field variables to the original ones. Afterward, the field variables can be used together with the evolution equations to evolve the physical system.

Given the linearity on the operators in CTT approach, the solutions can be thought as a superposition of solutions. The punctures method uses this feature to propose a

background conformal factor plus another solution which has to entail to the rest of the physical information.

Finally, in the third part we see that even when the constraint equations simplify with a flat conformal metric, for a boosted black hole in a trumpet geometry, the hamiltonian constraint has to be numerically solved. Given the BH linear momentum, the resulting equation has an axial symmetry along the momentum's direction.

The procedure of solving this equation is independent of which coordinates we use. Yet, the Bowen-York solution is given in cartesian coordinates and the differential operators simplify since the covariant derivatives reduce to partials. However, the solution's region implies a high numerical cost, not only by the complicated dependence of the radius in the background conformal factor, but because of the mesh of the grid has to be very fine in order to properly cover the region.

We found the geometry for some time slice, however, we cannot say anything about the evolution of the physical system. This is because the spacetime is the whole set of time slices threaded by the gauge conditions, and not just one. Therefore, the physical implications are uncertain at the bottom line. However, our solutions for the hamiltonian constraint, under punctures method, are in agreement with [IB09]. Even when this was the main objective, in our journey we noticed that this work may be the beginning for others.

The natural next step is evolving the system in time. Therefore, in order to get a good evolution a more precise inversion for the $r_{sch}(r)$ should be developed. The usage of the $r_{sch}(r)$ series in the background conformal factor increase the range of the solution and lead to more acceptable initial conditions. Even though, the number of needed iterations became the twice. Thus, we expect that using a numerical inversion to get $r_{sch}(r)$ would take many more iterations in order to solve properly the hamiltonian constrain.

In [BS10] is suggested that for a weak gravitational field the conformal factor is

easily related to newtonian potential. Therefore, a consequent analysis in simulations for particles orbiting around the BBH can be made.

We worked with the maximal slicing and zero shift vector conditions. Most of the publications about this subject use them because those conditions were the first ones to lead to the trumpet geometry. However, in recent papers they also use a modified harmonic slicing. This gamma of choices comes from the freedom to choose a reference frame and how it's changing along the time. From the perspective of GR, that is a small drawback since the usage of tensors in GR releases us from the exhaustive task of finding a good coordinate set. In spite of this, NR has allowed us to broaden our understanding of more realistic physical systems.

Appendices

Appendix A. Conventions and notation

Throughout this work we are using the following conventions and assumptions:

- Geometric units
$$c = G = k = 1\,. \tag{A.1}$$
- Metric signature $(-1, 1, 1, 1)$. This leads to negative magnitude for time-like vectors and positive for space-like vectors.
- Sum over repeated indices in ranges a - h and o - z runs from 0 to 3 otherwise they run from 1 - 3.
- We are following the tensor notation of [BS10]. That is a variation from [Wal84]. The indices in expressions not only stand for operative reasons but they are also attached to the objects giving them their meaning. For instance:
  - A^{ij} is a 3D-rank-2 tensor.
  - $\nabla_a T_{bc}$ is not only the derivative operator ∇ acting on T_{bc}, but also a 4D-rank-3 tensor.
- Vectors are denoted in two ways: Either with an arrow over or like rank-1 contravariant tensors.

For simplicity we are taking the metric tensor g^{ab} as the solution to Einstein's equations. The metric tensor is embedded in a 4D-smooth manifold that we call spacetime. In

addition, g^{ab} implies an isomorphism, i.e., vectors (one-forms) have their dual objects as one-forms (vectors)

$$v_a = g_{ab} v^b \,. \tag{A.2}$$

This leads to the commonly called indices' gymnastic. A result of using (A.2) is that there are only one v_a and dot product

$$(\vec{u}, \vec{v}) = g_{ab} u^a v^b = u^a v_a = u_a v^a \,. \tag{A.3}$$

In addition, we suppose that the solutions to Einstein's equations are torsion free. Therefore, the Christoffel symbols are symmetric [HEL06]:

$$\Gamma^a_{bc} = \Gamma^a_{cb} \,. \tag{A.4}$$

This, however, is argued to be unnecessary in order to develop 3+1 numerical relativity equations [Alc08, p.70].

Appendix B. Using Mathematica for calculations

B.1 Obtaining the terms $\bar{A}_0^2$, $\bar{A}_p^2$ and $\bar{A}_{0p}^2$

Here we are visiting a simple way of using *xAct* package in Mathematica to calculate the components of tensors and manipulate them to obtain terms (3.10). Since this is not an user's guide we recommend visiting [Me] (also is useful the discussion group [xAc]) for deeper information. We stress that this package is useful for Mathematica's versions 8.0 and above.

In *xAct* package most of Mathematica's objects are handled with rules instead of definitions. Tensors are used like scalar functions with integer arguments. Functions with *negative* (*positive*) symbols in their arguments mean they have covariant (contravariant) indices, e.g.

$$\texttt{A[-a,b]} \quad \rightarrow \quad A_a{}^b\,,$$

and indeed, the latter is the way Mathematica displays those objects.

To start we have to load the package xAct and its library *xCoba* which help us to use the objects' components. This is made with the command <<`xAct`xCoba`. This package uses automatically the `DollarIndices notation`. It specifies indices by giving them an particular number. However useful it is for Mathematica's inner calculations, it also

is jarring. We could turn off this with `$PrePrint=ScreenDollarIndices`.

Now, the first is to define the manifold's spacetime. It's defined as follows

```
DefManifold[M,4,IndexRange[a,q]] ,
```

where, M is its name; 4 its dimension and `IndexRange` implies that a to q indices are fixed to this metric. The later is useful for defining other objects like metrics or tensors. Lets define a metric `g` and chart associated to `M` by the indices

```
DefMetric[-1, metric[-a, -b], CD, PrintAs -> "g"];
DefChart[B, M, {0, 1, 2, 3}, {t[], r[], \[Theta][], \[Phi][]}];
```

here we defined `g` with signature -1 and a covariant derivative `CD` attached to it. On the other hand, we have defined the chart `B` representing the spherical coordinates. To fill in metrics' components it is useful defining first a matrix which actually has the metric's components we want to fill. For example, in flat metric the components are

```
MatrixForm[
 Minkowskisph = {{-1, 0, 0, 0}, {0, 1, 0, 0}, {0, 0, r[]^2, 0},
 {0, 0,0, r[]^2 Sin[\[Theta][]]^2}}]
```

$$\begin{pmatrix} -1 & 0 & 0 & 0 \\ 0 & 1 & 0 & 0 \\ 0 & 0 & r^2 & 0 \\ 0 & 0 & 0 & r^2 \sin^2\theta \end{pmatrix}.$$

And we pass those components to `g` employing chart `B` using the command `MetricInBasis` as follows

```
MetricInBasis[metric,-B, Minkowskisph]; MetricCompute{[metric, B, All, CVSimplify -> Simplify]};
```

Once defined `g[-a,-b]`, lets continue with the induced metric, γ^{ij}. Since the goal is to use the conformal metric $\bar{\gamma}^{ab}$, and it also is orthogonal to g^{ab}, we are dropping the over bar notation. This is not a problem because, as we see below, we are filling in γ^{ab}

with γ^{ab}'s components and the used operators do not involve conformal relations.

To define γ^{ab} we need to specify an orthogonal time-like vector, namely `u`. This is made with the option `InducedFrom` in `DefMetric` command

```
DefTensor[u[a], M]; u /: u[a_] u[-a_] := -1;
DefMetric[-1, metric\[Gamma]sph[-a, -b], cd, SymbolOfCovD -> {"\[Del]", "|"},
 PrintAs -> "\[Gamma]", InducedFrom -> {metric, u}]
```

Similar to `g[a,b]`, γ^{ij} has to be filled from an already defined matrix with γ^{ij}'s components

```
MatrixForm[
 Minkowskisph\[Gamma] = {{0, 0, 0, 0}, {0, 1, 0, 0}, {0, 0, r[]^2, 0},
 {0, 0, 0, r[]^2 Sin[\[Theta][]]^2}}];
MetricInBasis[metric\[Gamma]sph, -B, Minkowskisph\[Gamma]];
```

On the other hand, to define the traceless part of the extrinsic curvature tensor, $\bar{A}_0^{ij}$, we neeed the mass parameter, `M`, and the outgoing vector $\vec{l}$, c.f. (3.6). Using `v[j]` for the later

```
 DefConstantSymbol[Mass, PrintAs -> "M"]; DefTensor[v[a], M, OrthogonalTo -> u[-a]];
v /: v[a_] v[-a_] := 1; DefTensor[A0[i, j], M];
```

The association of `A0[i,j]` to its expression is given by

```
  A0[i, j] = (3*Sqrt[3]*Mass^2)/(4*r[]^3)*(metric\[Gamma]sph[i, j] - 3 v[i] v[j])  ,
```

but displayed like

$$\frac{3\sqrt{3}\mathrm{M}^2(\gamma^{ij} - 3v^i v^j)}{4r^3}\,.$$

The components of `v[i]` are passed with the function `AllComponentValues`

```
AllComponentValues[v[{i, B}], runit]/.runit = {1, 0, 0, 0};
ComponentValue[v[{0, B}]]
```

$$v^{\{0,B\}} \to 1\,,$$

where the index means that it's the $0th-$ component of `v[i]` in `B` chart. Finally, contracting `A0[i,j]` with its lowered indices version we have the $\bar{A}_0^2$ term. This is made by means of the commands `ToCanonical` and `ContractMetic`

```
A0[i, j] A0[-i, -j] // ToCanonical // ContractMetric
```

$$\frac{81M^4}{8r^6}\,.$$

In order to calculate the $\bar{A}_p^2$ term we define the momentum `p[j]` and its magnitude `P0` as follows:

```
DefTensor[P[i], M, OrthogonalTo -> u[-i]];
DefConstantSymbol[Momentum, PrintAs -> "P0"];
```

thus, defining $\bar{A}_p^{ij}$ as (3.2) and with `A1[i,j]` for it

```
DefTensor[A1[i, j], M];
A1[i, j] =  3/(2*r[]^2)*(P[i] v[j] + P[j] v[i] - (metric\[Gamma]sph[i, j]
            - v[i] v[j])*v[-k] P[k]);
```

it is displayed like:

$$\frac{3(v^iP^j + P^iv^j - P^k(\gamma^{ij} - v^iv^j)v_k)}{2r^2}\,.$$

In order to get the $\bar{A}_p^2$ we need to establish the rule for dot product of $\{\vec{P},\vec{P}\}$. With this we have that the contraction is

```
RulePM = IndexRule[P[j_] P[-j_], Momentum^2];
A1[i, j] A1[-i, -j] // ToCanonical // ContractMetric/. RulePM
```

$$\frac{9P_iv^iP_jv_j}{4r^4}+\frac{9P^iv_iP_jv^j}{4r^4}-\frac{9P^iv_iP^kv_k}{4r^4}-\frac{9P_iv^iP^kv_k}{4r^4}+\frac{9P^jv_jP^kv_k}{4r^4}+\frac{9P_jv^jP^kv_k}{4r^4}+\frac{9(P^kv_k)^2}{2r^4}+\frac{9P0^2}{2r^4}\,,$$

however, till this point Mathematica does not know that $P^iv_i = P_iv^i$. Once we have defined it, and that $P^iv_i = P0\cos\theta$, the contraction ends as (3.10c);

```
DotProdpv = IndexRule[P[i_] v[-i_], P[-j] v[j]];
%% /. DotProdpv;
RuleAngle = IndexRule[P[i_] v[-i_], P0*Cos[\[Theta][]]];
%% // Simplification/. RuleAngle //Simplify
```

$$\frac{9\left(P^k\right)^2\left(v_k\right)^2 + P0^2 + P0^2\cos^2(\theta)}{2r^4}\,.$$

For the remaining term, as we have defined all its needs, it is obtained as

```
A0[i, j] A1[-i, -j] // ToCanonical // ContractMetric
```

$$-\frac{27\sqrt{3}M^2P0\cos(\theta)}{4r^5}\,.$$

B.2 Solving the hamiltonian constraint

In this section we endeavor ourselves to solve (3.16):

$$\bar{D}^2u^{N+1} = -\frac{1}{8}\left(\psi_0 + u^N\right)^{-7}\bar{A}^2 + \frac{1}{8}\psi_0^{-7}\bar{A}_0^2 + \frac{7}{8}\psi_0^{-8}\bar{A}_0^2\left(u^{N+1} - u^N\right)\,. \tag{B.1}$$

For this purpose we use a second order center FDM. To do so, we use a discrete mapping from the interest region to a grid representing it, see figure B.1. Points of the solution are evaluated in positive integers indices $\{i, j\}$ in the grid, $u_{i,j}$. For the mapping we use the following rule:

$$x[i\_] = \Delta\mathtt{x}\,i + \mathtt{x0} \quad \text{and} \quad y[j\_] = \Delta\mathtt{y}\,j + \mathtt{y0}\,, \tag{B.2}$$

where $\Delta\mathtt{x} = \frac{\mathtt{Lx}}{\mathtt{Mx}}$, $\Delta\mathtt{y} = \frac{\mathtt{Ly}}{\mathtt{My}}$, $\mathtt{x0} = -\frac{\mathtt{Lx}}{2}$ and $\mathtt{y0} = -\frac{\mathtt{Ly}}{2}$. The parameters $\mathtt{Lx} = \mathtt{Ly}$ and $\mathtt{Mx} = \mathtt{My}$ are the sphere's diameter and the number of points along it, respectively. The above implies that $\mathtt{x0} = \mathtt{y0}$ corresponding to the center point in the grid. In this way the shaded region in the figure B.1 is where the obtained solution lies. The solution's region is actually poor for a small `Mx` but we hope that it fits better to the interest region as we increasing the grid points.

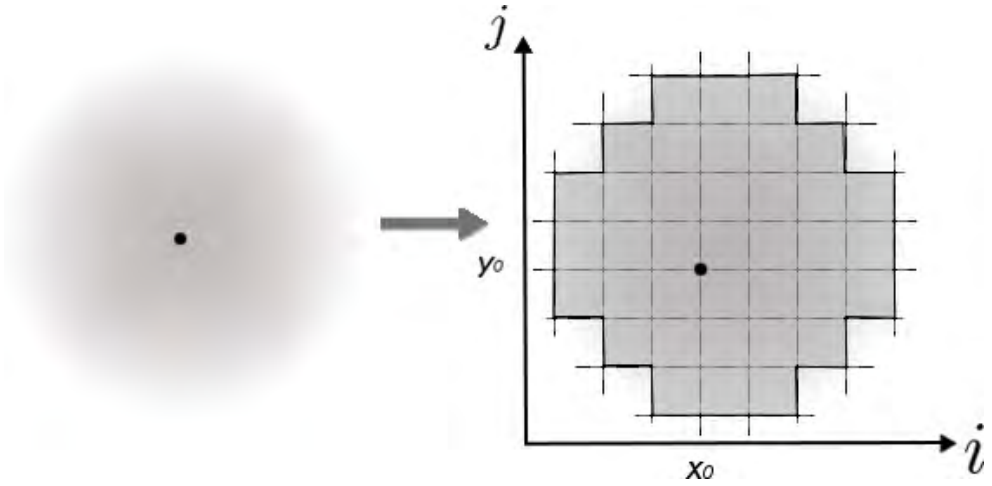

Figure B.1: Mapping to solution's region.

Using Mathematica for this calculation has the advantage that we could define the equations and variables for each point as items in lists. In this way we use the function `Solve` to obtain the value for each variable. This procedure avoids the reordering of the points' equations in a matrix and then invert it to find the values for the unknown variables. To do so, we have to define each unknown variable. This is made with the definition of the boundary functions:

$$f[j\_] := \texttt{Round}\left[\frac{1}{\Delta \texttt{x}}\left(-\texttt{x0} - \sqrt{(\texttt{Lx}/2)^2 - y[j]^2}\right)\right] \tag{B.3}$$

$$g[j\_] := \texttt{Round}\left[\frac{1}{\Delta \texttt{x}}\left(-\texttt{x0} + \sqrt{(\texttt{Lx}/2)^2 - y[j]^2}\right)\right] . \tag{B.4}$$

The functions `f` and `g` describe the left and right frontiers, respectively. The `Round` function takes the closest integer value for its argument. Unlike to `Floor` or `Ceiling`, this function leads to an symmetric distribution for the points in the grid. Then, we define the list for unknown variables as follows:

$$\texttt{vars} = \texttt{Flatten}\left[\texttt{Table}\left[\texttt{Table}\left[u_{i,j}^{N+1}, \{i, f[j]+1, g[j]-1\}\right], \{j, 1, \texttt{My}-1\}\right]\right] . \tag{B.5}$$

For example, with `Mx` $= 8$, we have the distribution's points in the figure B.2a. It doesn't seem to fill the whole circumference, however it helps to write the code for solving the equations.

{{4,0}}
{{1,1},{2,1},{3,1},{4,1},{5,1},{6,1},{7,1}}
{{1,2},{2,2},{3,2},{4,2},{5,2},{6,2},{7,2}}
{{0,3},{1,3},{2,3},{3,3},{4,3},{5,3},{6,3},{7,3},{8,3}}
{{0,4},{1,4},{2,4},{3,4},{4,4},{5,4},{6,4},{7,4},{8,4}}
{{0,5},{1,5},{2,5},{3,5},{4,5},{5,5},{6,5},{7,5},{8,5}}
{{1,6},{2,6},{3,6},{4,6},{5,6},{6,6},{7,6}}
{{1,7},{2,7},{3,7},{4,7},{5,7},{6,7},{7,7}}
{{4,8}}

(a) Points $\{i, j\}$ are distributed on the solution's region for $\texttt{Mx} = 8$.

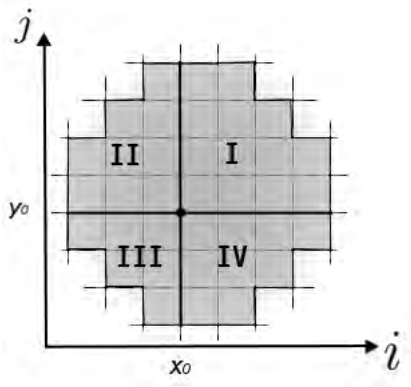

(b) Sections for the solution's region.

In order to define a list for the equations, lets recall that in section 2.3 we assumed conformal flatness, then the operator $\bar{D}^2$ is the Laplacian in Cartesian coordinates, $\bar{D}^2 \to \nabla^2$. Thus, we can cast it into (B.1) by differences between $u_{i,j}$ and its neighbors. The resulting equation is the one for inner points:

$$\begin{aligned} \frac{u^{N+1}_{i+1,j} - 2u^{N+1}_{i,j} + u^{N+1}_{i-1,j}}{\Delta \mathtt{x}^2} \;+\; & \frac{u^{N+1}_{i,j+1} - 2u^{N+1}_{i,j} + u^{N+1}_{i,j-1}}{\Delta \mathtt{y}^2} - \frac{7}{8}\psi 0^{-8}_{i,j} A0^{-2}_{i,j} u^{N+1}_{i,j} \\ = \;& -\frac{1}{8}\left(\psi 0_{i,j} + u^N_{i,j}\right)^{-7} A^2_{i,j} + \frac{1}{8}\psi 0^{-7}_{i,j}\left(1 - \frac{7u^N_{i,j}}{\psi 0_{i,j}}\right) A0^2_{i,j} \\ & \text{for} \quad f[j] < i < g[j] \quad \text{and} \quad 1 \le j \le \mathtt{My} - 1\,, \end{aligned} \tag{B.6}$$

where

$$r[j\_, k\_] := \sqrt{x[i]^2 + y[j]^2 + \epsilon^2}\,. \tag{B.7}$$

ϵ is a positive infinitesimal value to avoid numerical divergences. Notice that in equation (B.6), objects like $u_{i,j}$ should be entered in Mathematica as `u[i,j]`. Defining the left/right hand side as `LHS/RHS` the list for the equations follows as:

$$\mathtt{eqns} = \mathtt{Flatten}\left[\mathtt{Table}\left[\mathtt{Table}\left[\mathtt{LHS} == \mathtt{RHS}, \quad \{i, f[j] + 1, g[j] - 1\}\right], \{j, 1, \mathtt{My} - 1\}\right]\right] \tag{B.8}$$

This command implies that we have already defined the boundary points, e.g., when $i = f[j] + 1$ the equation (B.6) uses $i = f[j]$. In order to define these points we use the boundary condition (3.17) as follows:

$$\begin{aligned} \partial_r (ru) &\approx r_{i+1,j+1}\, u^{N+1}_{i+1,j+1} - r_{i-1,j-1} u^{N+1}_{i-1,j-1} \\ u^{N+1}_{j\pm1,k\pm1} &\approx \left(1 - \frac{\Delta \mathtt{x}}{r_{j\pm1,k\pm1}}\right) u^{N+1}_{j\pm1,k\pm1}\,, \end{aligned} \tag{B.9}$$

where $\pm$ depends on which section the boundary point is. From (B.9) we see that boundary points depend on the previous radial points. However, the use of this condition as clear in cartesian coordinates. To do so, we divide the solution's region in four parts as we see in figure B.2b. Then, we assume that the points' distribution is:

$$\begin{aligned} I &: \tfrac{\mathtt{Mx}}{2} \le i \le g[j] \quad \text{and} \quad \tfrac{\mathtt{My}}{2} \le j \le \mathtt{My} & II &: f[j] \le i \le \tfrac{\mathtt{Mx}}{2} \quad \text{and} \quad \tfrac{\mathtt{My}}{2} \le j \le \mathtt{My} \\ III &: f[j] \le i \le \tfrac{\mathtt{Mx}}{2} \quad \text{and} \quad 0 \le j \le \tfrac{\mathtt{My}}{2} & IV &: \tfrac{\mathtt{Mx}}{2} \le i \le g[j] \quad \text{and} \quad 0 \le j \le \tfrac{\mathtt{My}}{2} \end{aligned}$$

In addition, we choose the signs for the previous points in (B.9) as:

$$\begin{aligned} \{i,j\} &\to \{i-1, j-1\} \quad \text{for} \quad I \\ \{i,j\} &\to \{i+1, j-1\} \quad \text{for} \quad II \\ \{i,j\} &\to \{i+1, j+1\} \quad \text{for} \quad III \\ \{i,j\} &\to \{i-1, j+1\} \quad \text{for} \quad IV\,. \end{aligned}$$

With this choice, middle grid points don't take their previous points along the axis, see figure B.2b, however this kind of errors will be reduced as we increase `Mx`.

Once we define the boundary points, we use the command

$$\mathtt{Sol} = \mathtt{Solve}\,[\mathtt{eqns}, \mathtt{vars}]\,[[1]]\ . \tag{B.10}$$

to solve for the variables and if this is the first time it doesn't enter in a comparison to a minimal expected error

$$\mathtt{Do}\left[\mathtt{Do}\left[uc[i,j] = u^{N+1}[j,k]\mathtt{/.}\quad \mathtt{Sol}, \{i, f[j]+1, g[j]-1\}\right], \{j, 1, \mathtt{My}-1\}\right]\ .$$

Finally, if the minimal error is achieved we make an interpolation with the required precision to represent the solution.

Appendix C. u nearby solution

This appendix is dedicated to solving (3.12) using FSLT. First, since we have assumed flat conformal space, we recast the equation in the form

$$\nabla^2 u - \frac{7}{4r^2} u = f(r,\theta)\,, \tag{C.1}$$

where r is the conformal radius, $f(x,y) = \frac{1}{\sqrt{2}}\left(\frac{M}{r}\right)^{\frac{3}{2}} \frac{P\cos\theta}{M^3}$ and ∇^2 is the laplacian operator. We have dropped the bar over in the notation because all the expressions are conformal, otherwise we are indicating it.

This method is based in using the Sturm Liuville Problem to transform the differential equation. From (C.1) we identify the equation for Legendre's polynomials. Expanding the Laplacian in spherical coordinates and using the change of variable $x = \cos\theta$ we have

$$\partial_r\left(r^2\partial_r u\right) + \partial_x\left[\left(1-x^2\right)\partial_x u\right] = r^2 f(r,x) + \frac{7}{4}u \quad (-1 \le x \le 1)\,, \tag{C.2}$$

where the homogeneous equation corresponds to Legendre's polinomials $P_l(x)$. Then, with the transformation

$$\hat{u}_l(r) = \int_{-1}^{1} P_l(x) u(r,x) dx\,, \tag{C.3}$$

the solution to (C.1) is the linear combination of those u_l expanded with $P_l(x)$'s as basis functions

$$u(r,x) = \sum_{l=0}^{\infty} \frac{\hat{u}_l(r) P_l(x)}{\left|P_l(x)\right|^2}\,. \tag{C.4}$$

After multiplying (C.1) by $P_l(x)$ and integrating in x's interval we have

$$\left(r^2\bar{u}_l'(r)\right)' + \int_{-1}^{1} \partial_x \left[\left(1-x^2\right)\partial_x u(r,x)\right] P_l(x)dx = r^2 \int_{-1}^{1} f(r,x)P_l(x)dx + \frac{7}{4}\bar{u}_l(r)\,,$$

where the prime means derivative respect to r. We can invoke the SLP for the second term to have

$$\left(r^2\bar{u}_l'(r)\right)' - \lambda_l^2\hat{u}_l(x) = r^2\frac{\beta}{r^{\frac{3}{2}}}\int_{-1}^{1} xP_l(x)dx + \frac{7}{4}\bar{u}_l(r) \quad ; \quad \beta = \frac{P}{\sqrt{2}M^{\frac{3}{2}}}\,.$$

Using the orthogonal properties of $P_l(x)$ we arrive at the transformation of (C.1)

$$\left(r^2\bar{u}_l'(r)\right)' - l(l+1)\hat{u}_l(x) - \beta N_1 r^{\frac{1}{2}}\delta_{l,1} - \frac{7}{4}\bar{u}_l(r) = 0\,, \tag{C.5}$$

with N_l the normalization constant. In addition to the above equation we have the transformed boundary condition at $r = 0$

$$\bar{u}_l(0) = 0\,. \tag{C.6}$$

The solutions for (C.5) are in table (C.1). They are determined up to a constant

l	$\hat{u}_l(r)$
0	$c_0 r^{\sqrt{2}-\frac{1}{2}}$
1	$-\frac{1}{3}N_1\beta r^{\frac{1}{2}} + c_1 r^{\frac{3}{2}}$
$m \geq 2$	$c_m r^{-\frac{1}{2}+\sqrt{2+m(m+1)}}$

Table C.1: Transformed solutions

since we do not have information about $u(\vec{r})$ in r's middle range. The solution is obtained by means of (C.4)

$$\begin{aligned} u(\vec{r}) = \frac{c_0}{N_0}r^{\sqrt{2}-\frac{1}{2}}P_0(\cos\theta) \;&-\; \frac{\beta}{3}r^{\frac{1}{2}}P_1(\cos\theta) + \frac{c_1}{N_1}r^{\frac{3}{2}}P_1(\cos\theta) \\ &+\; \sum_{m=2}^{\infty}\frac{c_m}{N_m}r^{-\frac{1}{2}+\sqrt{2+m(m+1)}}P_m(\cos\theta)\,. \end{aligned}$$

Absorbing the normalization constant in the coefficient, the solution is expressed

$$u(\vec{r}) = -\frac{P}{3\sqrt{2}M^{\frac{3}{2}}}r^{\frac{1}{2}}\cos\theta + \sum_{m=0}^{\infty} C_m r^{-\frac{1}{2}+\sqrt{2+m(m+1)}}P_m(\cos\theta)\,. \tag{C.7}$$

This equation could help us to determine u's main behavior around the puncture.

Bibliography

[AAA+16] B. P. Abbott, R. Abbott, T. D. Abbott, M. R. Abernathy, F. Acernese, K. Ackley, C. Adams, T. Adams, P. Addesso, R. X. Adhikari, and et al. Observation of Gravitational Waves from a Binary Black Hole Merger. *Phys. Rev. Lett.*, 116(6):061102, February 2016.

[Alc08] M. Alcubierre. *Introduction to 3+1 Numerical Relativity*. Oxford University Press, 2008.

[BH10] B. Bassett and R. Hlozek. *Baryon acoustic oscillations*, page 246. Cambridge University Press, 2010.

[BHS99] Thomas W. Baumgarte, Scott A. Hughes, and Stuart L. Shapiro. Evolving einstein's field equations with matter: The "hydro without hydro" test. *Phys. Rev. D*, 60:087501, Sep 1999.

[BM94] R Beig and N Ó Murchadha. Trapped surfaces in vacuum spacetimes. *Classical and Quantum Gravity*, 11(2):419, 1994.

[BMSS95] Carles Bona, Joan Mass, Edward Seidel, and Joan Stela. New formalism for numerical relativity. *Phys. Rev. Lett.*, 75(4):600–603, 1995.

[BN07] Thomas W. Baumgarte and Stephen G. Naculich. Analytical representation of a black hole puncture solution. *Phys. Rev. D*, 75:067502, Mar 2007.

[BS10] T. W. Baumgarte and S. L. Shapiro. *Numerical Relativity: Solving Einstein's Equations on the Computer*. Cambridge University Press, June 2010.

[BY80] Jeffrey M Bowen and Jr. York James W. Time asymmetric initial data for black holes and black hole collisions. *Phys.Rev.*, 21(2047):2047–2056, 1980.

[Cha13] Eduardo WV Chaves. *Notes on Continuum Mechanics (Lecture Notes on Numerical Methods in Engineering and Sciences)*. Springer, 2013.

[Cho07] Dale Choi. Lectures on numerical relativity. `http://pelusa.fis.cinvestav.mx/tmatos/LaSumA/LaSumA2_archivos/RelatividadNum/Choi_Course/`, June 2007. accessed:February 2018.

[DED20] F. W. Dyson, A. S. Eddington, and C. Davidson. A determination of the deflection of light by the sun's gravitational field, from observations made at the total eclipse of may 29, 1919. *Philosophical Transactions of the Royal Society of London A: Mathematical, Physical and Engineering Sciences*, 220(571-581):291–333, 1920.

[ERI54] A. CEMAL ERINGEN. The finite sturm-liouville transform. *The Quarterly Journal of Mathematics*, 5(1):120–129, 1954.

[GGB02] E Gourgoulhon, P Grandclément, and S Bonazzola. Binary black holes in circular orbits. I. A global spacetime approach. *Phys. Rev. D*, 65(4):44020, feb 2002.

[GMG06] Carsten Gundlach and José M. Martín-García. Well-posedness of formulations of the Einstein equations with dynamical lapse and shift conditions. *Phy. Rev. D*, 74(2):1–19, 2006.

[Gou07] E. Gourgoulhon. 3+1 Formalism and Bases of Numerical Relativity. `http://adsabs.harvard.edu/abs/2007gr.qc.....3035G`, March 2007. Accessed: 2018-02-15.

[GP-a] GP-A was the launch of a precise clock on a suborbital rocket to explore the structure of space and time. `https://funphysics.jpl.nasa.gov/technical/grp/grav-probea.html`. Accessed: 2017-05-29.

[GP-b] GP-B. gravity probe b, launched 20 april 2004, is a space experiment testing two fundamental predictions of einstein's theory of general relativity (gr), the geodetic and frame-dragging effects, by means of cryogenic gyroscopes in earth orbit. `https://einstein.stanford.edu/highlights/status1.html`. Accessed: 2017-05-29.

[Gre98] W. Greiner. *Classical electrodynamics*. Electrodynamics. Springer-Verlag New York, Inc., 1998.

[HECB03] M. D. Hannam, C. R. Evans, G. B. Cook, and T. W. Baumgarte. Can a combination of the conformal thin-sandwich and puncture methods yield binary black hole solutions in quasiequilibrium? *Physical Review D*, 68(6):064003, September 2003.

[HEL06] M.P. Hobson, G.P. Efstathiou, and A.N. Lasenby. *General Relativity: An Introduction for Physicists*. Cambridge University Press, 2006.

[HHM09] Mark Hannam, Sascha Husa, and Niall Ó Murchadha. Bowen-york trumpet data and black-hole simulations. *Phys. Rev. D*, 80:124007, Dec 2009.

[IB09] Jason D. Immerman and Thomas W. Baumgarte. Trumpet-puncture initial data for black holes. *Phys. Rev. D*, 80(6):1–5, 2009.

[Lag04] P. Laguna. Conformal-thin-sandwich initial data for a single boosted or spinning black hole puncture. *Physical Review D*, 69(10):104020, May 2004.

[Me] J. Martín and et al. xAct is a suite of free packages for tensor computer algebra in mathematica. `http://www.xact.es/index.html`. Accessed: 2017-22-08.

[MTW73] C.W. Misner, K.S. Thorne, and J.A. Wheeler. *Gravitation*. W. H. Freeman, 1973.

[SN95] Masaru Shibata and Takashi Nakamura. Evolution of three-dimensional gravitational waves: Harmonic slicing case. *Phys. Rev. D*, 52:5428–5444, Nov 1995.

[SY78] L. Smarr and J. W. York, Jr. Kinematical conditions in the construction of spacetime. *Physical Review D*, 17:2529–2551, May 1978.

[TW89] J. H. Taylor and J. M. Weisberg. Further experimental tests of relativistic gravity using the binary pulsar PSR 1913 + 16. *Astrophysical Journal*, 345:434–450, October 1989.

[Wal84] R.M. Wald. *General Relativity*. University of Chicago Press, 1984.

[xAc] Google xAct group is a space for questions, answers and discussions about xact mathematica's package. `https://groups.google.com/forum/#!forum/xact`. Accessed: 2017-15-09.